(Volume to commemorate the Sixtieth Birthday
of Professor Sir Nevill Mott F.R.S.)

CHAPTER I

ELECTRONIC STRUCTURE OF METALS*

Volker Heine

*Supported in part by the National Aeronautics and Space Administration, U.S.A.

1.1 PSEUDISM

'Electronic structure', interpreted widely, covers all that the outer conduction electrons in metals do, and with it practically all solid state properties, in the sense that the energy of a vacancy for example is given in terms of the energy of the whole electronic system. The present chapter is concerned with electronic structure that can be treated theoretically from a 'fundamental' point of view, i.e., based on the solution of the Schrödinger equation with more or less well-defined and justifiable approximations. The theory of magnetism and of transport properties come within this definition, and form separate chapters. Otherwise, until recent years, it was only the band structure $\mathcal{E}(\underset{\sim}{k})$ of an electron with wave vector $\underset{\sim}{k}$ travelling through the periodic potential that could be discussed from fundamentals, together with a few immediately related properties such as the electronic specific heat. A phonon spectrum had to be analyzed in terms of ad hoc force constants. Now, however, it can be calculated in favourable cases from the same basic potential set up for computing $\mathcal{E}(\underset{\sim}{k})$. For simple metals, the area that can be treated 'fundamentally' is still centred on the band structure, but has begun to expand.

The concept unifying much of what we have to say is that of the pseudopotential. While the term is relatively new in the present context, some of the ideas it draws together predate it

qualitatively by twenty years. Recent developments sharpen and exploit them.

Figs 1 and 2 show the results of measurements on the Fermi surface of lead (Anderson and Gold 1965). The arcs of circles are what the Fermi surface would be for perfectly free electrons, namely the Fermi sphere cut up by Brillouin zone planes (fig. 1), the pieces being translated by appropriate reciprocal lattice vectors $\underset{\sim}{g}$ and reassembled in successive bands $\mathcal{E}_n(k)$ inside the fundamental Brillouin zone (fig. 2). The observed Fermi surface can be recognized as a modest distortion from the free electron model, and the same is true of all other metals studied except the transition, rare earth and actinide metals with incomplete inner d or/and f shells (see Ch. 2). Moreover the distortions conform qualitatively and sometimes quantitatively, to what would be expected on the basis of the nearly free electron (NFE) approximation.* The band structures of the group IV semiconductors diamond, Si, Ge, gray Sn and the III-V compounds have been probed by optical interband transitions, and the band structures inferred from the measurements also interpreted in NFE terms (see for example, Brust 1964, Cohen and Bergstresser 1966). Fermi surface measurements coupled with band structure calculations on the semimetals As, Sb, Bi indicate a NFE situation

*Throughout this chapter we shall not define terms that may easily be tracked down through the index of J. M. Ziman, Principles of the Theory of Solids, briefly referred to as Z.

there, too (Cohen, Falicov and Golin 1964, Priestley et al 1966, Lin and Falicov 1966, Falicov and Lin 1966). While the Fermi surface studies and optical properties provide detailed information about a part of the band structure, the soft X-ray emission spectra give a rough overall picture which in bandwidth and shape conforms approximately to free electrons.

Although most of the detailed evidence for the NFE picture has been built up in the last ten years, the beginnings can already be seen in Mott and Jones' (1936) treatment of diamond and bismuth, for example, in NFE terms.

The success of the NFE model for the band structure $\mathcal{E}(\underset{\sim}{k})$ does not imply, however, that the potential $V(\underset{\sim}{r})$ in the solid is weak or can be treated by perturbation theory, as assumed in most textbook presentations of the NFE method. $V(\underset{\sim}{r})$ becomes very strong near the atomic nuclei, much larger than the bandwidth of the conduction electrons and far too strong to be treated as a perturbation. Inside the ion core of the metal atom $V(\underset{\sim}{r})$ is a sufficiently deep potential well to produce several atomic-like oscillations in the wave function (fig. 3).

The applicability of the NFE model <u>does</u> mean that the net scattering by an atom is weak. In the augmented plane wave (APW) or Korringa-Kohn-Rostocker (KKR) formulation of the band structure problem, each ion core is surrounded by a sphere of radius R (fig. 4). $\mathcal{E}(\underset{\sim}{k})$ is determined by solving the Schrödinger equation in the Swiss-cheese-like interstitial region, subject to a boundary condition on the spheres given by the radial derivative

of the wave function or the phase shift (Z. pp. 87-97). The inner potential enters only through the latter. We may picture the core of the atom as a black box (fig. 5) scattering plane waves weakly from $\underset{\sim}{k}$ to $\underset{\sim}{k} + \underset{\sim}{q}$, and can introduce a weak pseudopotential $v(\underset{\sim}{q})$ [in Fourier transform] which acting on plane waves would produce just this same scattering.

How the scattering can be weak when the potential is strong follows from consideration of the phase shifts η_ℓ which we may write as

$$\eta_\ell = p_\ell \pi + \delta_\ell . \qquad (1.1)$$

The integer p_ℓ, chosen so that $|\delta_\ell| < \frac{1}{2}\pi$, counts the number of innter radial nodes. Since the usual phase shift formula for the scattering (Schiff 1955, p. 105) only involves exp 2 i η_ℓ, any multiple of π in (1.1) does not contribute and the scattering is determined by δ_ℓ which is relatively small. The pseudopotential therefore is a potential which has small phase shift δ_ℓ instead of the large η_ℓ, and is not strong enough to produce any oscillations of the corresponding pseudo wave function ϕ inside the core.

An explicit pseudopotential V_{ps} is given by (Austin et al 1962)

$$V_{ps}\phi = V\phi - \sum_c \langle \psi_c, V\phi \rangle \psi_c , \qquad (1.2)$$

where the ψ_c are the 1s, 2s, 2p, etc., orbitals in the ion core. (Strictly they are the 1s, etc., solutions of the same Hamiltonian that operates on the valence electrons and so may differ slightly from the actual orbitals of the core.) It is not difficult to show (Z. p. 97) that it gives the same valence eigenvalues in the pseudo wave equation*

---

*We use units with $2m = \hbar = e = 1$, except that energies will normally be given in Rydbergs where 1 Ry = 13.6 eV.

$$(-\nabla^2 + V_{ps})\phi = \mathcal{E}\phi \qquad (1.3)$$

as the real potential does. Since the ψ_c have definite angular momenta ℓ, the second term of (1.2) picks out and operates differently on the different ℓ components of ϕ. If we consider for a moment only the $\ell = 0$ component, ϕ is approximately a constant inside the core because radial oscillations have been eliminated and an s-state has no angular nodes, and so may be taken outside the matrix element in (1.4):

$$V_{ps}\phi \approx \left[V - \Sigma_c \langle \psi_c, V \rangle \psi_c\right]\phi. \qquad (1.4)$$

The $\langle \psi_c, V \rangle$ are the expansion coefficients of V in terms of the set ψ_c. If we had a complete set, the bracket in (1.4) would vanish identically. As it is, the ψ_c are a finite

set of core orbitals which form quite a good expansion set inside the core. Thus the second term in (1.4) cancels most of the strong potential V inside the core, as illustrated for a free Si^{4+} ion in fig. 6. In fact, (1.2) is a special case of a more general cancellation theorem developed by Phillips and Kleinman (1959), Cohen and Heine (1961), and Austin, Heine and Sham (1962).

Two points must be emphasized. The first is that a scattering amplitude from $\underset{\sim}{k}$ to $\underset{\sim}{k} + \underset{\sim}{q}$ depends in general not only on q but also on k, $|\underset{\sim}{k} + \underset{\sim}{q}|$ and the energy $\mathcal{E}$. The same applies to the pseudopotential, for example the nonlocal operator (1.2), and what we previously wrote as v(q) should be written

$$v(q; k, |\underset{\sim}{k}+\underset{\sim}{q}|, \mathcal{E}). \qquad (1.5)$$

Actually (1.2) does not have an explicit energy dependence but some forms of V_{ps} do, in particular those involving the logarithmic derivative or phase shift which vary with energy.

The second point is that the pseudopotential is weak compared with the real potential, too weak to produce radial oscillations in the pseudo wave function ϕ. In many cases it is in fact weak enough to make perturbation theory very useful for some problems, at least as a first step. But it is not always so weak that good answers can be calculated with the lowest order of perturbation theory to every question in solid state physics!

In many ways the pseudopotential approach represents a philosophy rather than a specific method: most calculations

that are done with it could be done equally well without ever using the word. But progress in science means unifying more and more experience through well-defined concepts which may be expressed in definite numbers. The pseudopotential serves that purpose for NFE metals. Ultimately most properties depend on the interaction of the conduction electrons with the ion cores, and so can be formulated in terms of $v(q)$. (See, for example, Harrison 1966). Some properties turn out to be rather sensitive to the small errors in $v(q)$ which even the best fundamental calculation contain. Here the principle of unifying knowledge suggests interpreting one set of experimental results in terms of another: a $v(q)$ may be fitted to the one and used to explain the other, or both may be shown consistent with a single $v(q)$.

1.2 BAND STRUCTURE CALCULATIONS

The various methods for calculating band structures have been described well in several texts (see e.g., Z. ch. 3, and Callaway 1964), and we will restrict ourselves to a few comments on the practical state of the art.

In a typical metal such as Al, the bandwidth is of the order of 1 Ry, the band gaps of order 0.1 Ry. An accuracy of 0.01 Ry in calculation is therefore highly desirable, and a few times 10^{-3} Ry for narrow bands such as in transition metals. The augmented plane wave (APW) and Korringa-Kohn-Rostocker (KKR) methods give a numerical accuracy of 10^{-3} Ry without difficulty, and they have been tested against each other by applying both to the same potential (Segall 1962, Burdick 1963). In the orthogonalized plane wave (OPW) method, convergence becomes very slow beyond about 0.01 Ry, because the representation of the inner oscillations of ψ in terms of plane waves and core functions ψ_c (Z. p. 94) is only an ad hoc "Ansatz" and it requires plane waves of very short wavelength to make the final corrections to ψ (Abarenkov and Heine, 1965). The success of the method depends on the fact that the Ansatz is remarkably good for atomic potentials which become progressively steeper near the origin. It does not work for a square well with infinitely high walls, for example. The OPW method has been tested against KKR (Segall 1961). The cellular method has in the past suffered from some

severe difficulties which Altmann and co-workers report to have overcome (Altmann 1958). So far there are no results which can be checked against existing KKR or APW calculations on exactly the same potential.

Band structure calculations have been done for a few compounds and stoichometric alloys, e.g., TiC, V_3Si with APW's (Ern and Switendick, Mattheiss 1965) and CuZn by the KKR method (Johnson and Amar 1965). Such work requires professionals. On the other hand, for a simple metal the KKR method is very easy to use, if the structure is bcc or fcc for which the required structure constants have been tabulated. Even for these the constants are only available along symmetry lines in the Brillouin zone, but these may serve to give quite a good picture of the band structure. Such calculations can be very useful as a guide in interpreting, for example, de Haas-van Alphen measurements (see ch. 2) on the Fermi surface. The OPW method is next in difficulty, still falling within the competence of an enthusiastic amateur. An APW calculation may take two years to develop from scratch. However, at least one experimentalist has learnt to use existing programmes to calculate a band structure as an aid in interpreting his data. The OPW and APW methods have been extended to include spin-orbit coupling, and in the case of APW all other relativistic effects (Weisz 1966, Loucks 1965a). The APW and KKR methods experience no difficulty with any kind of band structure but the OPW appears less suitable for narrow d (or f) bands such as in transition metals.

From §1, we can expand the Schrödinger equation in plane waves acted on by a pseudopotential, which will be relatively weak for NFE band structures. Indeed any secular equation of the form

$$\det \left\| \left\{ (\underset{\sim}{k}-\underset{\sim}{g})^2 - \mathcal{E} \right\} \delta_{\underset{\sim}{g}\underset{\sim}{g}'} + \Gamma_{\underset{\sim}{g}\underset{\sim}{g}'} \right\| = 0 \qquad (1.6)$$

can be interpreted that way with $\Gamma_{\underset{\sim}{g}\underset{\sim}{g}'}$ as the pseudopotential matrix elements. The OPW and APW methods fall in this category:

$$\Gamma_{\underset{\sim}{g}\underset{\sim}{g}'}\,(\mathrm{OPW}) = V_{\underset{\sim}{g}-\underset{\sim}{g}'} + \sum_c (\mathcal{E}-\mathcal{E}_c)\langle \underset{\sim}{k}-\underset{\sim}{g}|c\rangle\langle c|\underset{\sim}{k}-\underset{\sim}{g}'\rangle \qquad (1.7)$$

$$\Gamma_{\underset{\sim}{g}\underset{\sim}{g}'}\,(\mathrm{APW}) = (4\pi R^2/\Omega)\left\{ -\left[(\underset{\sim}{k}-\underset{\sim}{g})\cdot(\underset{\sim}{k}-\underset{\sim}{g}') - \mathcal{E}\right] \frac{j_1(|\underset{\sim}{g}-\underset{\sim}{g}'|R)}{|\underset{\sim}{g}-\underset{\sim}{g}'|} \right.$$

$$\left. + \sum_{\ell=0}^{\infty} (2\ell+1) P_\ell(\cos\theta_{\underset{\sim}{g}\underset{\sim}{g}'})\, j_\ell(|\underset{\sim}{k}-\underset{\sim}{g}|R)\, j_\ell(|\underset{\sim}{k}-\underset{\sim}{g}'|R)\, \frac{\mathcal{R}_\ell'(R,\mathcal{E})}{\mathcal{R}_\ell(R,\mathcal{E})} \right\}$$

(1.8)

(where $\theta_{\underset{\sim}{g}\underset{\sim}{g}'}$ is the angle between $\underset{\sim}{k}-\underset{\sim}{g}$ and $\underset{\sim}{k}-\underset{\sim}{g}'$, Ω the volume of the unit cell, and $\mathcal{R}'$

the derivative of the radial wave function R). Another one has been derived recently by Ziman (1965) from the KKR method:

$$\Gamma_{\underset{\sim}{g}\underset{\sim}{g}'}(\mathrm{KKRZ}) = -\frac{4\pi}{\varkappa\Omega}\sum_{\ell}(2\ell+1)\tan\eta_{\ell}'\,\frac{j_{\ell}(|\underset{\sim}{k}-\underset{\sim}{g}|R)\,j_{\ell}(|\underset{\sim}{k}-\underset{\sim}{g}'|R)}{j_{\ell}(\varkappa R)\,j_{\ell}(\varkappa R)}P_{\ell}(\cos\theta_{\underset{\sim}{g}\underset{\sim}{g}'}) \tag{1.9}$$

where $\cot\eta_{\ell}' = \cot\eta_{\ell} - n_{\ell}(\varkappa R)/j_{\ell}(\varkappa R)$, (1.10)

and $\varkappa^2 = \mathcal{E}$.

This formula presumably has the same excellent convergence in g,g' as the APW method because it is based in the same way on exact solution of the wave equation inside R. It is probably superior to Γ(APW) in that the summation over ℓ converges much more rapidly. Γ (APW) involves R_{ℓ} directly, which tends to the free spherical wave j_{ℓ} at large ℓ because the radial wave equation is dominated by the 'centrifugal term' $\ell(\ell+1)/r^2$, whereas Γ (KKRZ) depends through the phase shift only on the deviation of R_{ℓ} from j_{ℓ}. In fact, Morgan (1966) has shown that

$$\Gamma(\mathrm{APW}) = \Gamma(\mathrm{KKRZ}) + \Gamma^{0} \tag{1.11}$$

where Γ^0 is an 'empty lattice' term which however is not identically zero. This illustrates how the pseudopotential is not a unique quantity: any potential can be used which gives the correct phase shift or logarithmic derivative $\mathcal{R}'/\mathcal{R}$ at R.

Another pseudopotential, set up this time in r space, is simply a square well of depth A inside some model radius R_M and the appropriate Coulomb potential outside (fig. 7):

$$V_{ps}{}^{b} = -\sum_{\ell} A_{\ell}(E)\, P_{\ell}\,, \qquad r < R_M\,,$$

$$= -z/r \qquad\qquad r > R_M\,. \tag{1.12}$$

This is the pseudopotential of the bare ion core of charge z, to which has to be added the potential from the conduction electrons as detailed below. The well depth A can be adjusted so that (1.12) reproduces exactly the spectroscopically observed energy levels of one electron added to the ion (Abarenkov and Heine 1965). A depends on the angular momentum ℓ, and P_ℓ in (1.12) is a projection operator to pick out that component of the total wave function. A_ℓ also has to depend slightly on E to fit the whole series of levels of given ℓ. The matrix elements, between plane waves, of the nonlocal operator (1.12) can be calculated analytically without difficulty and inserted in the secular equation. The model radius R_M may be so chosen that there is little

discontinuity in V_{ps} at R_M, thus reducing the high Fourier components of V_{ps} as much as possible (Animalu and Heine 1965).

Incidentally, the eigenfunctions

$$\sum_{\underset{\sim}{g}} \alpha_{\underset{\sim}{g}} \exp i(\underset{\sim}{k}-\underset{\sim}{g})\cdot\underset{\sim}{r} \qquad (1.13)$$

of all these pseudopotential methods correctly represent the wave function $\psi_{\underset{\sim}{k}}$ in the region between the spheres (fig. 4) (Slater 1966, Morgan 1966).

Before any of these methods can be applied to calculate $\mathcal{E}(\underset{\sim}{k})$, the complete potential V or pseudopotential V_{ps} in the solid has of course to be set up. The potential of the ion core is often taken from a Hartree-Fock calculation. On the other hand, the use of a model potential such as (1.12) fitted to the spectroscopic energy levels has the advantage of automatically including exchange with the core orbitals and all internal correlation effects. In some cases, such as the d states in noble metals, a different functional form inside R_M has been found better than the square well. To obtain A_ℓ for $\ell \geq 1$ at the energy required in the solid, often entails some extrapolation from the atomic energy levels where A_ℓ has been determined, and this can introduce a little uncertainty in the method.

As regards the conduction electrons, often the potentials of neutral free atoms are taken and simply superposed. These are usually from Hartree-Fock-Slater calculations (HFS, with the Slater (1951) approximation for exchange), which have been pub-

lished for all elements. After this potential of superposed atoms has been constructed, it has to be averaged to spherical symmetry inside the radius R for use in the APW or KKR method. It is also approximated to by constant (some average value) between the spheres for the KKR method, while variations about this constant can be incorporated with APW's if desired. Exchange with the core and conduction electrons is then usually treated by the Hartree-Fock-Slater approximation. Although the procedure of superposing neutral atoms is somewhat arbitrary, it has yielded many useful answers (See, for example, Loucks 1965b). Herman (1964) has used OPW's to solve for the wave functions and made the whole potential self-consistent, again within the HFS scheme.

The use of pseudopotentials allows us to approach the whole problem of setting up a self-consistent potential for the conduction electrons in another way (Cohen and Phillips 1961). We first need the pseudopotential $V_{ps}{}^{b}$ of a bare ion, usually calculated from (1.7) or the model potential (1.12), though there is no reason why other forms should not be used. The next step is to treat the conduction electrons as a uniform negative jelly into which the ions are planted. The pseudopotential of the whole system is

$$(\text{const.}) + \sum_{\underset{\sim}{g}}{}' \, v^{b}(g) \exp i\underset{\sim}{g}\cdot\underset{\sim}{r} \qquad (1.14)$$

$$v^{b}(g) = \Omega^{-1} \int V_{ps}{}^{b} \exp(-i\underset{\sim}{g}\cdot\underset{\sim}{r}) \, d\underset{\sim}{r}. \qquad (1.15)$$

(We write $v^b(g)$, leaving the other variables of (1.5) understood.) The electron gas does not contribute to the Fourier components $v^b(g)$ in (1.14) becuase it is uniform. It only cancels the infinite g = 0 component which the ions alone would give. We now allow the conduction electrons to react with the 'bare' pseudopotential (1.14) and screen it. A Fourier component $\rho_{\underset{\sim}{g}}$ of the charge density is set up, proportional to the 'applied' potential $v^b(g)$ in lowest order of perturbation theory if we treat $v^b(g)$ as weak. (The method therefore only applies in NFE cases.) The result of a self-consistent calculation is to reduce $v^b(g)$ to

$$v(g) = v^b(g) / \epsilon(g) \tag{1.16}$$

where $\epsilon(g)$ is the appropriate screening factor or 'dielectric constant' (Z. pp. 126-9). The pseudopotential for the whole system is then

$$V = (\text{const}) + \sum'_{\underset{\sim}{g}} v(g) \exp i\underset{\sim}{g}\cdot\underset{\sim}{r} \tag{1.17}$$

The point is that since the pseudopotential acts on pseudo wave functions which are plane waves (before being perturbed), we can take $\epsilon(g)$ from the theory of the free electron gas. Such is the principle of the method, but there are several points of detail to be inserted. Since the $V_{ps}{}^b$ is nonlocal, the screening is not simply given by a multiplicative factor as in (1.16) and has to be calculated

nonlocally (Harrison 1963, Animalu 1965). The charge density of the conduction electrons is not uniform, even in lowest approximation, because of the oscillations of $\psi_{\underset{\sim}{k}}$ in the core (fig. 3), resulting in a reduced density there (the 'orthogonality hole') and a heaping up to a density $z(1 + \alpha)$ electrons per atom outside the core. Here α is the order of 0.1 and the effect may be incorporated with V_{ps}^{b} in (1.15). Exchange and correlation with the core electrons is included in V_{ps}^{b} of the ion. Exchange and correlation with the conduction electrons produces a hole which moves with the electron and contributes an exchange and correlation energy $\mu_{xc}(k)$ for the state k. To a first approximation it is uniform because the electron gas is uniform, but it fluctuates somewhat due to the charge density fluctuation $\rho_{\underset{\sim}{g}}$. That contribution can be included in (1.16), the best method at present probably being to calculated $\epsilon(g)$ with a short range screened exchange interaction treated in the Hubbard approximation (Sham 1963, 1965). We obtain

$$\epsilon(g) = 1 - (1+\alpha)\left(\frac{4\pi e^2 z}{\Omega g^2}\right)\left(1 - \frac{\frac{1}{2} g^2}{g^2 + k_F^2 + k_s^2}\right)\chi(g) \qquad (1.18)$$

where

$$\chi(g) = -\left(\frac{2}{3}\varepsilon_{F0}\right)^{-1}\left(\frac{1}{2} + \frac{4k_F^2 - g^2}{8 g k_F} \ln\left|\frac{2k_F - g}{2k_F + g}\right|\right). \qquad (1.19)$$

Here ε_{F0} is the free electron Fermi energy $\hbar^2 k_F^2/2m$.

~~where~~ The term [....] in (1.18) comes from the exchange and k_s is the screening parameter taken as $(2k_F/\pi)^{\frac{1}{2}}$ in atomic units. The effect of the orthogonality hole in modifying the screening is taken into account crudely by the factor $1 + \alpha$ in (1.18). These are small points. The usefulness of the dielectric screening method depends on the fact that $\epsilon(g) \rightarrow 1$ as $g \rightarrow \infty$ and is already of order 1.2 at the first reciprocal lattice vectors. Thus a 10°/o error in the screening, i.e., in $\epsilon(g) - 1$, results only in a 2°/o error in v(g) in (1.16). The $\mu_{xc}(k)$ can be calculated at the Fermi level from formulae for the total exchange and correlation of the electron gas. As nearly as theory or experiment can tell (10-20°/o, see for example, Pines 1955), $\mu_{xc}(k)$ may be taken as constant throughout the band. Finally there is a rather small and rather uncertain correlation correction which may be added, coming from the fact that correlation with core electrons and with conduction electrons is not additive as assumed implicitly so far. We merely mention these points to indicate how far it is possible now to treat all the interactions between nonlocality, self-consistency including the orthogonality hole, exchange and correlation (see, e.g., Animalu and Heine 1965, Harrison 1966). In one calculation on Si self-consistency, exchange and correlation were computed with the calculated Bloch functions (Phillips and Kleinman 1962).

A complete review of band structure calculations up to 1962 may be found in Callaway (1964), with its useful list of references including the titles of all the papers to serve as one-line abstracts. Some further calculations are listed by Heine (1965). A good general text is Slater (1965).

1.3 ANALYSIS OF NFE BAND STRUCTURES

In § 1 it was emphasized that the band structures of many metals and semiconductors can be described in NFE terms with a pseudopotential v(g) for scattering by a reciprocal lattice vector $\underset{\sim}{g}$. In § 2 we saw how to calculate v(g), but for really useful results one needs to achieve an accuracy of 0.01 Ry or better, which is difficult when one has cancellations between quantities inherently of magnitude 1 Ry in a complicated self-consistent many-body system. We shall therefore discuss the analysis of experimentally measured band structures to yield the 'observed' pseudopotential v(g). These pseudopotentials can then be correlated with atomic properties to describe trends in the band structures across the periodic table, or used to calculate other properties of the metals as in § 4.

A typical analysis is that of Harrison (1959) and Ashcroft (1963) on the Fermi surface of aluminium as determined by the de Haas-van Alphen effect (ch. 2). We start with the secular equation (1.6) of infinite order, where we shall now use v instead of Γ and sometimes write it for simplicity with a single argument $\underset{\sim}{g}-\underset{\sim}{g}'$ while remembering the full nonlocal nature (1.5). Only the {111} and {200} Brillouin zone planes cut the Fermi sphere, the others having only a minor effect on $\mathcal{E}(\underset{\sim}{k})$ near the Fermi energy $\mathcal{E}_F$. Around the corner $W_1 = (\pi/a)(2,0,1)$ of the Brillouin zone, only the plane waves $|\underset{\sim}{k} = \underset{\sim}{G}_n>$ with

$$\underset{\sim}{G}_1 = 0$$

$$\underset{\sim}{G}_2 = (\pi/a)(\bar{2},2,\bar{2})$$

$$\underset{\sim}{G}_3 = (\pi/a)(\bar{4},0,0)$$

$$\underset{\sim}{G}_4 = (\pi/a)(\bar{2},\bar{2},\bar{2}) \qquad (1.20)$$

mix strongly into the pseudo wave function ϕ_k becuase they lie near the corners W_1 to W_4 (fig. 8) and are nearly degenerate. We need only investigate $\mathcal{E}(\underset{\sim}{k})$ in 1/48th part of the zone around W_1 because of the cubic symmetry. We can therefore partition the secular equation

$$\left\| \begin{array}{c|c} \underset{\sim\sim}{hh'} & \underset{\sim\sim}{hG'} \\ \hline \underset{\sim\sim}{Gh'} & \underset{\sim\sim}{GG'} \end{array} \right\| = 0 \qquad (1.21)$$

where $\underset{\sim}{h}$ denotes a higher $\underset{\sim}{g}$ not of the set (1.20), and apply a transformation of the type

$$\begin{vmatrix} A & B \\ \tilde{B}^* & C \end{vmatrix} \times \begin{vmatrix} I & -A^{-1}B \\ -C^{-1}\tilde{B}^* & I \end{vmatrix} = \begin{vmatrix} A-BC^{-1}\tilde{B}^* & 0 \\ 0 & C-\tilde{B}^*A^{-1}B \end{vmatrix}. \qquad (1.22)$$

The original $AB\tilde{B}^*C$ secular equation (1.21) is split into two separate ones in the upper left and lower right corners. In this way we can fold the infinite secular equation (1.6), (1.21) into a 4x4 secular equation which gives the lowest four eigenvalues exactly. The terms may be evaluated by expanding the A^{-1} in (1.22) by perturbation theory:

$$\det \| \{(\underset{\sim}{k}-\underset{\sim}{G})^2 - \varepsilon\} \delta_{\underset{\sim}{G}\underset{\sim}{G}'} + \bar{v}_{\underset{\sim}{G}\underset{\sim}{G}} \| = 0 , \qquad (1.23)$$

$$\bar{v}_{\underset{\sim}{G}\underset{\sim}{G}'} = v_{\underset{\sim}{G}\underset{\sim}{G}'} + \sum_{\underset{\sim}{h}} \frac{v_{\underset{\sim}{G}\underset{\sim}{h}}\, v_{\underset{\sim}{h}\underset{\sim}{G}'}}{\varepsilon - (\underset{\sim}{k}-\underset{\sim}{h})^2} + \cdots \qquad (1.24)$$

$$v_{\underset{\sim}{g}\underset{\sim}{g}'} = \langle \underset{\sim}{k}-\underset{\sim}{g} | v(\varepsilon) | \underset{\sim}{k}-\underset{\sim}{g}' \rangle . \qquad (1.25)$$

The price that has to be paid for folding into a finite secular equation is that the second and higher order terms in (1.24) introduce a $\underset{\sim}{k}$ and ε dependence into the matrix elements of the secular equation. In the case of pseudopotentials such $\underset{\sim}{k}$ and ε dependence is there already, so nothing is lost if the corrections terms are small. For Al , Animalu (1965) calculated them to be about 0.005 Ry. For calculating the shape of the Fermi surface the ε dependence is immaterial since it is set equal to a

constant $\mathcal{E}_F$. [Incidentally, the $\mathcal{E}$ dependence of v(g) does contribute to the band gap which, at the centre of a zone face, is equal to

$$\mathcal{E}_s - \mathcal{E}_p = \langle -\tfrac{1}{2}\underset{\sim}{g} | v(\mathcal{E}_s) | \tfrac{1}{2}\underset{\sim}{g} \rangle + \langle -\tfrac{1}{2}\underset{\sim}{g} | v(\mathcal{E}_p) | \tfrac{1}{2}\underset{\sim}{g} \rangle , \tag{1.26}$$

where $\mathcal{E}_s$ and $\mathcal{E}_p$ are the s-like and p-like states at the band gap.]

The Fermi surface of Al was fitted with the 4x4 equation (1.23) with the $\bar{v}_{\underset{\sim}{G}\underset{\sim}{G}'}$ treated as local, i.e., a function of $|\underset{\sim}{G}-\underset{\sim}{G}'|$ only. Thus there were only two parameters which were found to have the values (Ashcroft 1963)

$$\bar{v}(111) = 0.0179 \text{ Ry}, \qquad \bar{v}(200) = 0.0562 \text{ Ry}. \tag{1.27}$$

The number of decimal places witnesses to the accuracy of the fit, much higher than one could expect from fundamental calculations except by chance. But it is at first sight very surprising that such a good fit was obtained with constant $\bar{v}$ matrix elements in view of the considerable nonlocality of v(g) (fig. 9). The reason is that a particular $\bar{v}_{\underset{\sim}{G}\underset{\sim}{G}'}$ only has a major effect on the shape of the Fermi surface when $\underset{\sim}{k}-\underset{\sim}{G}$, $\underset{\sim}{k}-\underset{\sim}{G}'$ are both near the Fermi

level, i.e., when the scattering by $\underset{\sim}{G}$-$\underset{\sim}{G}'$ is nearly between two points on the Fermi sphere. The values (1.27) represent $\bar{v}_{\underset{\sim}{G}\underset{\sim}{G}'}$ for that geometry (fig. 10).

In a study of Si and Ge (Brust 1964: see also similar work on compound semiconductors by Cohen and Bergstresser 1966) the band structures as inferred from optical and other data were fitted successfully using the ~~full~~ extended secular equation (1.6) with v(111), v(220), v(311) as three (constant) parameters and all higher $v_{\underset{\sim}{g}\underset{\sim}{g}'}$ set equal to zero. Again many of the matrix elements are probably quite spurious because of the real nonlocality, but as one calculates different bands and different $\underset{\sim}{k}$ particular matrix elements enter very strongly in a way similar to fig. 10 and the numerical values correspond to that situation.

As band structures become more precisely established, it is unlikely that fitting with constant matrix elements will suffice. This has already been found in Mg where there is a large amount of very precise de Haas-van Alphen data (Starke, private communication), and in Bi (Golin 1967). The need then arises for a model of the matrix elements with a small number of physically meaningful parameters. We can always split the pseudopotential (in $\underset{\sim}{r}$ space) into some mean local potential which acts equally on all ℓ components of ϕ, plus some nonlocal parts. The local part gives constant matrix elements and may be treated as before. Alternatively a simple one-parameter model has been found useful by Ashcroft (1967). The cancellation theorem and fig. 6 suggest we may take the bare pseudopotential of an ion as

zero inside some adjustable radius R_A which is nearly that of the ion core, and -z/r outside. We obtain

$$v_{loc,\,\underset{\sim}{G}\underset{\sim}{G}'} = -\frac{4\pi e^2 z}{\Omega g^2 \epsilon(g)} \cos(gR_A) \tag{1.28}$$

where $\epsilon(g)$ is the screening factor (1.18) and $g = |\underset{\sim}{G}-\underset{\sim}{G}'|$. A second parameter can of course be introduced by giving the well a depth as in fig. 7. The nonlocal part may be expressed as the deviation of the A_ℓ in (1.12) from the mean. By adjusting R_A we have chosen this mean to be zero, and if we regard only $\ell = 0$ and 1 as important at such small r, we may put

$$\begin{aligned} V_{nonloc} &= A(P_0 - P_1), \quad r < R_A, \\ &= 0, \quad r > R_A. \end{aligned} \tag{1.29}$$

We write

$$K = |\underset{\sim}{k}-\underset{\sim}{G}|, \qquad K' = |\underset{\sim}{k}-\underset{\sim}{G}'|,$$

$$x = KR_A, \qquad x' = K'R_A. \tag{1.30}$$

then the matrix elements of (1.29) for K=K' are

$$V_{\text{nonloc}\,\underset{\sim}{G}\underset{\sim}{G}'} = \frac{2\pi R_A^{\,3} A}{\Omega}\left\{[j_0(x)]^2 - x^{-1}\cos x\, j_1(x) - 3\left(1-\frac{q^2}{K^2}\right)\{[j_1(x)]^2 - j_0(x) j_2(x)\}\right\},$$

(1.31a)

and for $K \neq K'$

$$V_{\text{nonloc},\underset{\sim}{G}\underset{\sim}{G}'} = \frac{4\pi R_A^{\,2} A}{\Omega\,[K^2-K'^2]}\left\{K j_1(x) j_0(x') - K' j_1(x') j_0(x) - 3\left(\frac{K^2+K'^2-q^2}{2KK'}\right)\{K j_2(x) j_1(x') - K' j_2(x') j_1(x)\}\right\}.$$

(1.31b)

There is no reason why R_A in the local and nonlocal parts should be exactly the same. If the $\ell = 2$ potential is thought to be unusually strong, such as in Ca and perhaps K just before the 3d transition series (Vasvari, Animalu and Heine 1967), then we can take the $\ell = 2$ potential as the local one and write instead of (1.29)

$$V_{\text{nonloc}} = A P_0 - A' P_1, \quad r < R_A. \qquad (1.32)$$

In (1.31) the first two terms in the curly bracket must then be multiplied by A and the remainder by A'.

As already described, the Fermi surface of Al was fitted by a folded 4x4 secular equation with $\bar{v}$ matrix elements, whereas the band structure of Si with a large (essentially infinite order)secular equation and matrix elements of v. The former has the advantage of smaller size and incorporation of some higher order correction in an effective matrix element. The arbitrariness of the pseudopotential (subject always of course to its being a valid pseudopotential) results in varying behaviour for v(g) at large g. By summing up some of this into what is a partial t-matrix (1.24), one has included higher order Born approximations and arrived at a more invariant quantity, since all pseudopotentials must give the same final scattering and band structure. If the summation in (1.24) is extended over all $\underset{\sim}{g}$, it defines in fact the t-matrix. However, the use of a small finite secular equation also has two disadvantages. Firstly the correction terms in (1.24) and $\bar{v}$ depend to some extent on the structure considered, whereas v is the pseudopotential for one screened atom, so that there is some error in transferring values of $\bar{v}$ found by fitting the Fermi surface in one structure to another situation. Secondly the 4x4 secular equation is only good near W. At K in the zone (fig. 8), there are three plane waves in the lowest degenerate set, and two $(\pi/a)(-5/2,0,3/2)$, $(\pi/a)(3/2,0,-5/2)$ in the next highest set of which only the former is included in the four k-G's. In principle the $\underset{\sim}{k}$ dependence of the higher

order corrections in the $\bar{v}$ matrix elements compensates for this, but in practice such an asymmetry is a serious drawback and Melz (1966) could not get an unambiguous fit to his measurements on the change of Fermi surface around K with pressure.

We conclude it may be better to use a large secular equation with v matrix elements, than a reduced one with $\bar{v}$ elements. In that case there is a problem because (1.28), (1.31) do not drop off very rapidly at high $\underset{\sim}{g}$'s due to the discontinuities in the potentials V_{ps}^{b} assumed in real space. We may remedy this by assuming instead a smoothed pseudopotential

$$\int V_{ps}^{b}(\underset{\sim}{r}')\ F(\underset{\sim}{r}-\underset{\sim}{r}')\, d\underset{\sim}{r}' \qquad (1.33)$$

where F is a Gaussian smoothing function. The effect on the matrix elements (1.28), (1.31) is to multiply them by D(g), the Fourier transform of F, which is also a Gaussian

$$D(g) = \exp(-Bg^2). \qquad (1.34)$$

The limited experience at present suggests v(g) can be taken to cut off at about $3k_F$, and B may be chosen accordingly.

Spin orbit coupling V_{SO} may be included by writing

$$\langle \underset{\sim}{k}-\underset{\sim}{G}, \nu | V_{SO} | \underset{\sim}{k}-\underset{\sim}{G}', \nu' \rangle$$

$$= i \Lambda\, \underset{\sim}{S}_{\nu\nu'} \cdot (\underset{\sim}{k}-\underset{\sim}{G}) \wedge (\underset{\sim}{k}-\underset{\sim}{G}') \qquad (1.35)$$

where ν, ν' denote the components of the Pauli spin matrices s_x, s_y, s_z. Somewhat more complicated expressions may be derived from OPW's (Weisz 1966) or the square-well model potential (Animalu 1966).

The band structures change systematically both with valency z and within one column of the periodic table. Since only a fraction of the pseudopotentials have been determined experimentally, we show the trends from the calculated v(g), which however have been found in fair agreement with observed ones for several metals. Table 1 gives the approximate hypothetical band gaps

$$\mathcal{E}_s - \mathcal{E}_p \approx 2\, v(g) \tag{1.36}$$

for the z = 2 and 3 metals if they occurred in the bcc structure with their normal atomic volume. (This structure was chosen because the Brillouin zone is bounded by only one type of zone face, the $\{110\}$.) We note the z = 3 band gaps are systematically lower than the z = 2 ones. This reflects the fact that the ion cores of the z = 3 atoms are smaller relative to the atomic radii, making gR_A in (1.28) small and mostly less than $\frac{1}{2}\pi$ so that v(g) is negative. Within elements of the same z, $\mathcal{E}_s - \mathcal{E}_p$ decreases as the atomic number Z increases in accordance with the lowering of the s-state relative to the p-state in the free atoms (Cohen and Heine 1958, Austin and Heine 1966, Heine 1966).

1.4 OTHER ELECTRONIC PROPERTIES OF NFE METALS

The total energy and behaviour of metallic systems is almost entirely determined by the conduction electrons. In NFE metals their interaction with the ions is completely describable by the pseudopotential. We might therefore hope to formulate in terms of v(q) everything from the energy of a vacancy to the scattering of electrons in a liquid metal, from the electron-phonon interaction to the structure of alloys. Indeed some progress along these lines is slowly being made (Harrison 1966).

We may formulate the total pseudopotential in the system for an arbitrary set of atomic sites $\underset{\sim}{s}_n$ in the manner of (1.17):

$$V(\underset{\sim}{r}) = (\text{const}) + \sum_{\underset{\sim}{q}}{}' S(\underset{\sim}{q})\, v(q) \exp i\underset{\sim}{q}\cdot\underset{\sim}{r} \quad , \tag{1.37}$$

$$S(\underset{\sim}{q}) = (1/N) \sum_n \exp(-i\underset{\sim}{q}\cdot\underset{\sim}{s}_n), \tag{1.38}$$

where N is the total number of atoms in the system and $S(\underset{\sim}{q})$ the same structure factor as in X-ray or neutron diffraction. There is no difficulty generalizing (1.37) to more than one atomic species.

In order to make further progress we clearly need to know v(q) as a function of q. We have shown in §2 how it may

be calculated, but have emphasized repeatedly in §§ 2 and 3 that it is difficult to achieve the last 0.01 Ry or so in accuracy though this is important for the applications. The wise thing is therefore to let nature tell us the answer and take v(q) from an analysis of, say, the observed Fermi surface determined from de Haas-van Alphen measurements in the manner of § 3. This is illustrated for aluminium in fig. 11. The two points on the right are the values (1.27) at the (111) and (200) reciprocal lattice vectors, and the point at q = 0 is

$$v(0) = -3/\mathcal{N}(\varepsilon_F) \tag{1.39a}$$

$$\approx -\frac{2}{3}\varepsilon_{FO} \tag{1.39b}$$

fixed by basic theory (Z. pp. 130, 177). Here $\mathcal{N}(\varepsilon_F)$ is the density of states at the Fermi level per atom, and ε_{FO} the free electron Fermi energy. A whole curve for v(q) was calculated from fundamentals. It missed passing through v(111) and v(200) by 0.01 Ry, and was then adjusted slightly to fit them. We may therefore take this as a reliable interpolation of v(q) from the observed points (fig. 11)(Ashcroft and Guild 1965).

The resistivity of molten aluminium can now be calculated. It is proportional to (ch. 6)

$$\int_0^{2k_F} |S(q)|^2 |v(q)|^2 q^3 \, dq \tag{1.40}$$

where $S(q)\, v(q)$ is the matrix element of the potential (1.37) for scattering by wave vector q. Here $|S(q)|^2$ for the liquid was taken directly from X-ray measurements, and excellent agreement with the observed resistivity was obtained (Ashcroft and Guild 1965). It is important to observe that in (1.40) one needs the matrix element of the nonlocal pseudopotential relevant to scattering on the Fermi sphere, and this is precisely the geometry to which the experimentally determined points v(111) and v(200) on fig. 11 relate, as shown in fig. 10. In fact many properties of metals are concerned with processes around $\mathcal{E}_F$, for example the resistivity of the solid at high temperature due to phonon scattering, and the enhancement of the effective mass at low temperature by the electron-phonon interaction ($\S$ 1.5). Both these were calculated for Al and good agreement with experiment obtained (Ashcroft and Wilkins 1965). The self-consistently determined potential (1.15), (1.16), (1.37) solves then the old question of 'rigid ion' versus 'deformable ion' in the electron-phonon interaction (Sham and Ziman 1963). The pseudopotential moreover becomes the intermediate vehicle for interpreting one set of properties in terms of another. A further example is the deformation potential in Si calculated by Kleinman (1963) with the OPW form.

The success of such calculations depends of course on the transferability of v(q) between one material and another. A rather more drastic test of this was made for Sb. The pseudopotential of Sb, as determined from the optical properties of

InSb, was used to calculate the band structure of Sb semimetal. In antimony several bands are nearly degenerate around $\mathcal{E}_F$ and a good starting approximation for v(q) is necessary to obtain even qualitatively a unique picture. Only small adjustment of v(q) was required to fit the observed Fermi surface (Falicov and Lin 1966). In transferring pseudopotentials a correction should be made for change in atomic volume, the Ω^{-1} in (1.15). Also $\epsilon(q)$ in (1.16) depends on the electron density. For indium in InSb, should one take the mean density of four electrons per atom, or just three? These are nonlinear effects not included in the simple dielectric screening method: it is probably best to take a density of three electrons. Fig. 12 shows v(q) for indium determined by Cohen and Bergstresser (1966) from the optical properties of InP, InAs, InSb, after scaling to the atomic volume of indium metal but without adjusting the screening. There is clearly some scatter about a smooth curve indicating variations in the screening. More remarkable is the smallness of the variation. Part of the explanation is that $\epsilon(q)$ is about 1.1 to 1.2 for these q's, so that the valence electron density already contributes little, and variations in environment have only very small effect. Paragraph 9 We now discuss the total energy U of the whole system up to second order in the pseudopotential, and its application to various properties. To lowest order we treat the atomic polyhedron as a sphere of radius R_a and the electrons as a free electron gas, or rather single OPW's with an orthogonality hole. This energy U_0, which we shall discuss further in § 7, depends

only on the volume of the system, not the atomic positions $\underset{\sim}{s}_n$. We are here interested in the structure dependent energy of atomic rearrangements at constant volume. It is (see, e.g., Cohen 1962, 1963; Harrison 1963, 1966; Sham 1963; Blandin 1963; Pick and Sarma 1964; Heine and Weaire 1967)

$$U_S = U_E + \sum_{\underset{\sim}{q}} |S(\underset{\sim}{q})|^2 [v(q)]^2 \beta(q) \chi(q). \tag{1.41}$$

Here U_E is the Ewald or Fuchs (1935) energy of point ions of charge z* in a uniform negative background, less $-0.9\ z^{*2}e^2/R_a$ already included in U_0. The remainder of (1.41) comes from second order perturbation theory applied to (1.37) and we shall define β and χ as we derive it. The largest contribution to U_S is the sum of one-electron energies $\varepsilon(\underset{\sim}{k})$. The second order contribution to $\varepsilon(\underset{\sim}{k})$ from a single $\underset{\sim}{q}$ is

$$\frac{|S(\underset{\sim}{q})\, v(q)|^2}{\underset{\sim}{k}^2 - (\underset{\sim}{k}+\underset{\sim}{q})^2}. \tag{1.42}$$

This has to be summed over all occupied states inside the Fermi surface, which to second order may be taken as the unperturbed Fermi sphere. We obtain

$$|S(\underset{\sim}{q})\, v(q)|^2\, \chi(q) \tag{1.43}$$

where χ is the perturbation characteristic

$$\chi(q) = \sum_{k<k_F} \frac{1}{\underset{\sim}{k}^2 - (\underset{\sim}{k}+\underset{\sim}{q})^2} \tag{1.44}$$

whose value has already been given in (1.19). As is well known in Hartree-Fock theory, certain electrostatic and exchange terms have to be subtracted from the sum of the eigenvalues $\mathcal{E}(\underset{\sim}{k})$, as otherwise they would be counted twice in the total energy U. That is the origin of β in (1.41). When exchange and correlation in the total energy are treated by the Hubbard-Sham approximation (Sham 1963, 1965), it turns out β is the same as ϵ (1.18), but this would not be so in a more complete many-body treatment. Summation over $\underset{\sim}{q}$ then gives (1.41).

In the step from (1.42) to (1.43), we have treated $|Sv|$ as a constant factor and applied the summation only to the denominator. Since v(q) is in fact nonlocal, this is an approximation which need not be made but is not as serious as might at first appear (see Harrison 1966, p. 43). In (1.44), all terms with $\underset{\sim}{k}$ and $\underset{\sim}{k}+\underset{\sim}{q}$ both inside the Fermi sphere cancel exactly since they correspond to mixing wave functions inside the single Slater determinant. The largest contributions to (1.41), (1.43) comes when the energy denominator goes to zero at the limiting point where $\underset{\sim}{k}$ is just inside and $\underset{\sim}{k}+\underset{\sim}{q}$ just outside the Fermi sphere. The error is therefore not large if we take v(q) for scattering on the Fermi sphere as before, and we shall term this the limit-

ing point approximation. The reader is referred to Harrison (1966) and Kleinman (1966) for various details concerning the contribution of the orthogonality hole, exchange, etc. to $\hat{U}$.

One of the most fruitful applications of (1.41) has been to the calculation of phonon spectra (Sham 1963). The phonon frequency is simply a measure of the energy of a lattice wave distortion. Fig. 13 shows one recent such calculation for A (Animalu, Bonsignori and Bortolani 1966), computed from a pseudopotential based on the model (1.12) and quite close to fig. 11. With the same pseudopotential Hodges (1967) has calculated the stacking fault energy of Al as 195 ergs cm^{-2} compared with the experimental value 280 ± 50 ergs cm^{-2} (Edington and Smallman 1965).

All workers have found that the results of such calculations depend rather sensitively on v(q). The mean structural weight $|S(q)|^2$ in q-space is given simply by the mean atom density, and any structural change merely shifts it around. One is effectively differentiating $[v(q)]^2$. Moreover there is always a cancellation between the two terms in (1.41), leaving a net small quantity. The Ewald term always opposes distortions from a regular symmetrical structure, whereas the band structure term reduces this since it describes the screening by the electron gas. A pseudopotential fitted to two experimental points as in fig. 11 leaves open considerable uncertainties particularly about the behaviour at large q and the nonlocal corrections. There is also doubt about the exchange and correlation energy in $\beta(q)$,

and the orthogonality hole. The most fruitful procedure may therefore be to consolidate all the uncertainties into

$$\Phi_{bs}(q) = [v(q)]^2 \beta(q) \chi(q). \qquad (1.45)$$

With a calculated or experimentally determined pseudopotential as starting approximation, $\Phi_{bs}(q)$ can be fitted to the measured phonon spectra, and then applied to stacking fault calculations, phase changes (§7), and the structure of liquids (Johnson et al 1964).

The energy (1.41) may be Fourier transformed to an effective pair potential $\Phi(r)$ between ions (Cohen 1962, Harrison 1966):

$$\Phi(r) = -\frac{z^{*2}}{r} + \frac{\Omega}{\pi^2}\int_0^\infty \Phi_{bs}(q)\, r^{-1} \sin(qr)\, q\, dq. \qquad (1.46)$$

At large r it turns into the Friedel wiggles:

$$\Phi \sim (\text{const})\,[v(2k_F)]^2 \frac{\cos 2k_F r}{(2k_F r)^3}. \qquad (1.47)$$

In the present formulation, the asymptotic form (1.47) arises from the region $q \approx 2k_F$ in the integration (1.46), where χ has its most rapid variation (see § 7).

It corresponds therefore to neglecting the variation of v(q). Blandin (1966) has applied this approximation to stacking fault calculations, among other things, where the arrangement of nearest neighbours does not change. While Hodges (1967) has not found it a satisfactory approximation for detailed numerical calculation, it does give an illuminating picture of the broad trends with valency.

Everything so far has been based on perturbation theory and the assumption of a weak pseudopotential. In a regular crystalline structure, even a complicated one, this condition is satisfied, as it is too in a crystal distorted by a lattice wave or a stacking fault, because the atom density is very uniform. However in a vacancy, near an interstitial, or at a surface, the potential becomes strong due to the large v(q) at small q (fig. 11). ['Strong' and 'large' compared with v(q) at the reciprocal lattice vectors, not with bare atomic potentials.] Perturbation theory no longer suffices. It is necessary to solve for the t-matrix (Messiah 1961) and do the self-consistency calculation in terms of it. Bennemann has developed a new iteration procedure for calculation t especially for potentials peaked in q space aroung q = 0 as v(q) is (fig. 11), and applied it to problems of bond formation, work function, and formation and migration energies of vacancies and interstitials in group 4 semiconductors (Bennemann 1964, 1965).

1.5 LANDAU QUASI-PARTICLES

In metals the Coulomb interaction between conduction electrons is typically of order 1 Ry, quite comparable with the bandwidth. It is therefore at first sight surprising that a model of independent particles in one-electron Bloch orbitals $\psi_{\underset{\sim}{k}}$, such as we have been using, is at all relevant. The entity moving through the metal is an electron surrounded by a denuded region, the correlation and exchange hole. Its energy is defined by the zero of the inverse Green function $G_o^{-1}(\underset{\sim}{p},\underset{\sim}{r},\mathcal{E})$, and we can write a Schrödinger equation for the motion of the whole quasi-particle

$$(-\nabla^2 + V(\underset{\sim}{r}) + M - \mathcal{E})\psi = 0, \tag{1.48}$$

where M is the 'proper self energy' operator describing the exchange and correlation with the other conduction electrons. For a free electron gas it reduces to $\mu_{xc}(k)$ defined in § 2. Since the quasi-particle moves through a periodic medium, all the concepts of $\underset{\sim}{k}$ space, the Bloch theorem and Brillouin zones, remain valid.

There is, however, one qualification: the quasi-particle has a finite lifetime and the energy an imaginary component. There

is a residual screened Coulomb interaction between quasi-particles, so that a quasi-particle $\underset{\sim}{k}$ above the Fermi surface may collide with one $\underset{\sim}{k}_1$ in the Fermi sea which is scattered to $\underset{\sim}{k}_2$ while the original quasi-particle recoils to $\underset{\sim}{k}_3$. Both energy and momentum have to be conserved in the process, the former implying that $\underset{\sim}{k}_1$, $\underset{\sim}{k}_2$ and $\underset{\sim}{k}_3$ must all like within an energy $|\mathcal{E}(\underset{\sim}{k}) - \mathcal{E}_F|$ of the Fermi level where $\mathcal{E}(\underset{\sim}{k})$ is the original quasi-particle energy. This requirement puts a severe limitation on the range of collisions which are possible when $\mathcal{E} - \mathcal{E}_F$ is small, and the lifetime of the quasi-particle tends to infinity as $(\mathcal{E} - \mathcal{E}_F)^{-2}$. The Fermi surface itself is therefore perfectly sharp (Mott 1956), as is indeed found in the de Haas-van Alphen effect where features of the Fermi surface on the scale of 10^{-3} to 10^{-4} Ry may be studied. The effect is well known in the soft X-ray emission spectra where the cut off at the Fermi level is sharp, but the transitions from states near the bottom of the band are broadened of the order of 0.1 Ry. The broadening of states well above $\mathcal{E}_F$ is presumably comparable.

In many phenomena one is only concerned with low energy excitations very close to $\mathcal{E}_F$ produced by electric and magnetic fields and thermal excitation. For such situations the states of the whole electron system may be specified by a distribution $(f_{\underset{\sim}{k}} - f^\circ_{\underset{\sim}{k}})$ of quasi-particles just above $\mathcal{E}_F$ and quasi-holes just below. Here $f^\circ_{\underset{\sim}{k}}$ is the Fermi-Dirac distribution at T = 0, and we write the quasi-particle distribution as $(f_{\underset{\sim}{k}} - f^\circ_{\underset{\sim}{k}})$ to preserve similarity to the ordinary discussion of independent particles.

The total energy of the system (to second order in $f_{\underset{\sim}{k}} - f^{\circ}_{\underset{\sim}{k}}$) may be written (Landau 1956)

$$U = \sum_{\underset{\sim}{k}} \varepsilon(\underset{\sim}{k}) \, (f_{\underset{\sim}{k}} - f^{\circ}_{\underset{\sim}{k}}) + \tfrac{1}{2} \sum_{\underset{\sim}{k}\underset{\sim}{k}'} \eta(\underset{\sim}{k}, \underset{\sim}{k}') \, (f_{\underset{\sim}{k}} - f^{\circ}_{\underset{\sim}{k}})(f_{\underset{\sim}{k}'} - f^{\circ}_{\underset{\sim}{k}'}), \tag{1.49}$$

where $\eta(\underset{\sim}{k},\underset{\sim}{k}')$ represents the interaction energy of quasi-particles, and the variables $\underset{\sim}{k},\underset{\sim}{k}'$ are taken to include a specification of spin. Before we discuss the contribution of η to various properties, we must say precisely what we mean. As mentioned in §2 and in connection with (1.48), the one-quasi-particle energy $\varepsilon(\underset{\sim}{k})$ contains an exchange and correlation term $\mu_{xc}(\underset{\sim}{k})$ which was stated to be almost independent of $\underset{\sim}{k}$. This is true to within 10°/₀ for a NFE metal and in any case becomes a bit meaningless well below ε_F because of the lifetime broadening. However near ε_F where $\varepsilon(\underset{\sim}{k})$ is well defined, detailed calculations (Rice 1965 and references there) suggest that the k dependence of μ_{xc} for a free electron gas contributes up to 10°/₀ to the electron velocity $\partial\varepsilon/\partial\hbar k$. These are certainly many-body corrections but they are incorporated in the $\varepsilon(\underset{\sim}{k})$ and hence already included in the independent particle model. We are concerned with <u>further</u> corrections arising from the interaction $\eta(\underset{\sim}{k},\underset{\sim}{k}')$ in (1.49).

The best known example is the enhancement of the spin paramagnetism. The simple Pauli result $\mu_B^2 N(\varepsilon_F)$ for the

susceptibility counts only the single-quasi-particle energy $\mathcal{E}(\underset{\sim}{k})$ (Z. p. 286), whereas turning some spins over alters the total exchange energy of the system in a way that enhances the susceptibility. From (1.49) the susceptibility becomes

$$\chi = \frac{\mu_B{}^2 \mathcal{N}(\mathcal{E}_F)}{1 - \nu} \qquad (1.50)$$

where μ_B is the Bohr magneton, and

$$\nu = -\frac{2}{\mathcal{N}(\mathcal{E}_F)\ (2\pi)^6} \times \iint \frac{dS_{\underset{\sim}{k}}}{\partial\mathcal{E}/\partial k_n} \frac{dS_{\underset{\sim}{k}'}}{\partial\mathcal{E}/\partial k_{n'}} \left[\eta(\underset{\sim}{k}\uparrow, \underset{\sim}{k}'\uparrow) - \eta(\underset{\sim}{k}\uparrow, \underset{\sim}{k}'\downarrow)\right].$$

When $\partial\mathcal{E}/\partial k_n$ is small as in transition metals, ν may exceed unity, resulting in a formally infinite susceptibility and hence a spontaneous ferromagnetic polarization.

Another important application of (1.49) is to the electronic specific heat. In thermal equilibrium there are equal numbers of excited quasi-particle just above any element $dS_{\underset{\sim}{k}}$ of Fermi surface, and quasi-holes below. Their contributions exactly cancel in the second term of (1.49) and the electronic specific heat is given by the usual formula $\frac{1}{3}\pi^2 k^2 \mathcal{N}(\mathcal{E}_F)$ in terms of the one-quasi-particle density of states $\mathcal{N}(\mathcal{E}_F)$.

The energy of a quasi-particle may be considered modified in the molecular field sense by the interaction from the other quasi-

particles present:

$$\tilde{\mathcal{E}}(\underset{\sim}{k}, \underset{\sim}{r}) = \mathcal{E}(\underset{\sim}{k}) + (2\pi)^{-3}\int [f_{\underset{\sim}{k}'}(\underset{\sim}{r}) - f^{0}_{\underset{\sim}{k}}]\, \eta(\underset{\sim}{k}, \underset{\sim}{k}')\, d\underset{\sim}{k}' \qquad (1.51)$$

The local energy $\tilde{\mathcal{E}}$ of a quasi-particle may depend on $\underset{\sim}{r}$ since $f_{\underset{\sim}{k}}$ in general does, and we can define a 'local Fermi surface' or surface of equal chemical potential by $\tilde{\mathcal{E}}(\underset{\sim}{k},\underset{\sim}{r}) = \mathcal{E}_F$. As usual in transport theory, we write

$$f_{\underset{\sim}{k}}(\underset{\sim}{r}) - f^{0}_{\underset{\sim}{k}} = -\phi_{\underset{\sim}{k}}(\underset{\sim}{r})\ \partial f^{0}_{\underset{\sim}{k}} / \partial k_n \qquad (1.52)$$

where k_n is the component of $\underset{\sim}{k}$ normal to the Fermi surface. Then ϕ measures the distance in $\underset{\sim}{k}$ space that the Fermi surface has been distorted from equilibrium. Alternatively the quasi-particle distribution may be defined in terms of the distortion $\psi_{\underset{\sim}{k}}(\underset{\sim}{r})$ [not to be confused with the wave function ψ] from the 'local Fermi surface' (Heine 1962):

$$\psi_{\underset{\sim}{k}} = \phi_{\underset{\sim}{k}} + (8\pi^3 t\, v_{\underset{\sim}{k}})^{-1} \int \eta(\underset{\sim}{k}, \underset{\sim}{k}')\, \phi_{\underset{\sim}{k}'}\, dS_{\underset{\sim}{k}'}. \qquad (1.53)$$

The Boltzmann equation is

$$-\frac{\partial \phi_{\underset{\sim}{k}}}{\partial t}\frac{\partial f^{0}}{\partial k_n} - \underset{\sim}{v}_{\underset{\sim}{k}} \cdot \frac{\partial \psi_{\underset{\sim}{k}}}{\partial \underset{\sim}{r}}\frac{\partial f^{0}}{\partial k_n} + e\underset{\sim}{n}_{\underset{\sim}{k}} \cdot \underset{\sim}{E}\frac{\partial f^{0}}{\partial k_n} = \dot{f}_{\underset{\sim}{k}}\Big]_{\text{scattering}} \qquad (1.54)$$

(n_k is the unit normal on the Fermi surface.)

In order to solve it, one must express it completely in terms of ϕ or ψ, but we have written a hybrid form to exhibit each term at its simplest. The time-dependent term must depend on the complete quasi-particle distribution ϕ and not ψ, since $\tilde{\varepsilon}$ in terms of which ψ is defined also changes with time. The drift term however involves ψ because the other quasi-particles exert accelerations through $\eta(\underset{\sim}{k},\underset{\sim}{k}')$ which keep $\tilde{\varepsilon}$ constant. The scattering term involves $\phi_k/\tau(\underset{\sim}{k})$ in a relaxation time approximation since the relaxation is of the whole system to equilibrium. However, if we write a collision integral for elastic scattering, that depends on ψ since $\tilde{\varepsilon}$ is conserved (Silin 1958, Heine 1962).

The total current may be written

$$J = e(2\pi)^{-3} \int \underset{\sim}{v}_{\underset{\sim}{k}} \psi_{\underset{\sim}{k}} \, dS_{\underset{\sim}{k}} . \qquad (1.55)$$

In the case of time-independent processes, (1.54) and (1.55) in terms of ψ are formally identical with the equations in the independent quasi-particle model if we assume elastic scattering. There are then no Landau corrections to the transport properties. This conclusion still holds for thermal currents and in the presence of static magnetic fields, and applies for example to the Wiedemann-Franz law. Time-dependent transport properties in general do have corrections through the first term in (1.54). In the case of the anomalous skin effect, the corrections tend to zero in the extreme anomalous limit (Silin 1957) because the

displacement is such a sharp spike around the Fermi equator as pictured by the ineffectiveness concept (Z. p. 244). The same applies to the cyclotron frequency under Azbel-Kaner conditions, which remains as normally defined in terms of the Fermi velocity $\partial\mathcal{E}(\underset{\sim}{k})/\partial\hbar\,\underset{\sim}{k}$ (Z. pp. 250, 255). In the opposite limit when the electric field is uniform over the cyclotron orbit as realized in semiconductors, there are Landau corrections. It would be interesting if with ultrasonic waves one could cover the crucial range between the two extremes.

A more fundamental formula for the total current is

$$J = (2\pi)^{-3} \int \underset{\sim}{j}_{\underset{\sim}{k}} \, (f_{\underset{\sim}{k}} - f^{o}_{\underset{\sim}{k}}) \, d\underset{\sim}{k} \tag{1.56}$$

in terms of the current $\underset{\sim}{j}_{\underset{\sim}{k}}$ carried by a quasi-particle. This is not $e\,\underset{\sim}{v}_{\underset{\sim}{k}}$ but

$$\underset{\sim}{j}_{\underset{\sim}{k}} = e\Big[\underset{\sim}{v}_{\underset{\sim}{k}} + (8\pi^3 t)^{-1} \int \underset{\sim}{n}_{\underset{\sim}{k}'} \, \eta(\underset{\sim}{k}, \underset{\sim}{k}') \, dS_{\underset{\sim}{k}'} \tag{1.57}$$

In the case of a free electron gas, i.e., with interaction but zero periodic potential, the momentum of a quasi-particle must be $\hbar\,\underset{\sim}{k}$ and the current $(e/m)\hbar\,\underset{\sim}{k}$. Then (1.57) reduces to the Landau identity

$$\frac{1}{m} = \frac{1}{m^*} + \frac{k_F}{2\pi^2 t^2} \int_0^{\pi} \eta_s(\theta_{\underset{\sim}{k}\underset{\sim}{k}'}) \cos\theta \sin\theta \, d\theta, \tag{1.58}$$

and η_s is the mean interaction for parallel and antiparallel spins.) where $m^* = \hbar k/v$. This result means that for a free electron gas certain exact cancellations of many-body corrections can take place. For example, the 'semiconductor' cyclotron mass becomes the bare electron mass m, which is what the usual formula for the cyclotron mass would give if applied to the Hartree band structure $\hbar^2k^2/2m$ without the exchange and correlation terms $\mu_{xc}(k)$. That may partly explain why $\underset{\sim}{k}\cdot\underset{\sim}{p}$ perturbation theory is so successful in fitting the observed cyclotron masses in semiconductors because the $\underset{\sim}{k}\cdot\underset{\sim}{p}$ perturbation theory also breaks down for the exchange and correlation potential.

The $\eta(\underset{\sim}{k},\underset{\sim}{k}')$ considered so far is the screened Coulomb interaction. There is another one, the interaction via virtual phonons. As is well known since it is the origin of superconductivity, an electron moving through the lattice attracts the positive ions in its immediate neighbourhood, and their small displacement to the centre results in an attractive potential for other electrons. It contributes also to the self-energy $\mathcal{E}(\underset{\sim}{k})$, analogously to $\mu_{xc}(\underset{\sim}{k})$. At absolute zero of temperature we may write

$$\mathcal{E}(\underset{\sim}{k}) = \mathcal{E}_e(\underset{\sim}{k}) + \frac{1}{(2\pi)^3}\int \frac{|\mathcal{M}(\underset{\sim}{k},\underset{\sim}{k}+\underset{\sim}{q})|^2}{\mathcal{E}_e(\underset{\sim}{k}) - \mathcal{E}_e(\underset{\sim}{k}+\underset{\sim}{q}) - \hbar\nu_{\underset{\sim}{q}}}\, d\underset{\sim}{q} \qquad (1.59)$$

where $\mathcal{E}_e$ is the purely electronic energy and $\mathcal{M}$ the matrix element for emission of a phonon $\underset{\sim}{q}$ of energy $\nu_{\underset{\sim}{q}}$ with the electron

being scattered to $\underset{\sim}{k}+\underset{\sim}{q}$. If we consider $\underset{\sim}{k}$ just below the Fermi surface, the scattering can only contribute as in (1.44) if $\underset{\sim}{k}+\underset{\sim}{q}$ is an empty state above $\mathcal{E}_F$, the contribution being large only if $\underset{\sim}{k}$ and $\underset{\sim}{k}+\underset{\sim}{q}$ lie within Θ_D (the Debye temperature) of $\mathcal{E}_F$. The distortion of the band structure is shown in fig. 14. The reduction in the Fermi velocity is about 35% in Al, a factor of two in Pb, for example, as observed in the cyclotron mass and electronic specific heat (Ashcroft and Wilkins 1965). At high temperatures the effect disappears because with the thermal excitation of quasi-particles there are terms with positive energy denominator which cancel the negative ones. The general framework of the Landau theory still applies, even at finite temperature, and it turns out that time-independent transport processes are unaffected by the phonon contributions, i.e., the interaction $\eta(\underset{\sim}{k},\underset{\sim}{k}')$ cancels the effect of the distortion (fig. 14) of the single quasi-particle spectrum (Prange and Kadanoff 1964). The anomaly of fig. 14, being intimately connected with the discontinuity at the Fermi surface, rides up and down with $\mathcal{E}_F$ if the electron density is altered, which allows one to derive an identity between the reduction in $\partial\mathcal{E}/\partial k$ in the one-quasi-particle energy and the mean value of $\eta(\underset{\sim}{k},\underset{\sim}{k}')$ around the Fermi surface.

The reader is referred to Nozières (1964) for a general development of the Landau theory with referencesto the literature, to Prange and Kadanoff (1964) for its formulation with the phonon interaction, and to Heine, Nozières and Wilkins (1966) for a review of its application to the screening and scattering of pseudopotentials.

TABLE 1. Approximately band gaps 2v(g) for hypothetical bcc structures (in Ry.), from calculations by Animalu and Heine (1965).

Be	Mg	Zn	Cd	Hg
0.19	0.06	0.05	0.04	0.02

	Al	Ga	In	Tl
	0.05	-0.01	-0.03	-0.10

FIGURE CAPTIONS

Fig. 1 The free electron Fermi sphere (light) and the observed Fermi surface of lead (heavy), shown with Brillouin zone planes in extended $\underset{\sim}{k}$ space. (After Anderson and Gold 1965).

Fig. 2 Similar to fig. 1, but with the various parts of the Fermi surface joined together inside the fundamental Brillouin zone. (After Anderson and Gold 1965).

Fig. 3 Real wave function ψ and pseudo wave function ϕ of an electron in a NFE metal. R_c is the radius of the ion core.

Fig. 4 (No comment)

Fig. 5 The pseudopotential v(q) defined in terms of the scattering amplitude of an atom, pictured as a black box, for scattering of electrons from $\underset{\sim}{k}$ to $\underset{\sim}{k}+\underset{\sim}{q}$.

Fig. 6 The potential and pseudopotential (for $\ell = 0$ states) of a Si^{4+} ion. The potential V is expressed in the form $V(r) = Z(r)/r$ and V_{ps} similarly in terms of $Z_{ps}(r)$. Note V and V_{ps} both become equal to the Coulomb potential

$-4/r$ outside the core which has a radius of about one Bohr unit. (After Cohen and Heine 1961).

Fig. 7 A model pseudopotential for an ion of charge z.

Fig. 8 Brillouin zone for face centred cubic lattice, showing points of high symmetry.

Fig. 9 Pseudopotential v(q) for aluminium, showing its non-local nature. The top and bottom curves are for backward and forward scattering respectively ($\underset{\sim}{k}$ and $\underset{\sim}{k}+\underset{\sim}{q}$ parallel and antiparallel in eq. 1.5), whereas the middle curve is for scattering on the Fermi sphere as in fig. 10. (After Animalu, private communication).

Fig. 10 Scattering on the Fermi sphere.

Fig. 11 Pseudopotential of aluminium.

Fig. 12 Pseudopotential v(q) for indium, as fitted from ● InP, ■ InAs, and + InSb, all scaled to the atomic volume of metallic indium, and × from indium metal. The curve is calculated from the model potential (1.12) and (1.16). (After Animalu and Heine 1965).

Fig. 13 Calculated (continuous curve) and measured (circles) phonon spectrum of aluminium. (After Animalu et al 1966).

Fig. 14 Effect of electron interaction via virtual phonons on the band structure near the Fermi level at absolute zero of temperature.

Fig. 15 Band structure of copper (schematic).

Fig. 16 The perturbation characteristic $\chi(q)$, eq. (1.19), (1.44), in units of $\frac{2}{3}\mathcal{E}_{F0}$

Fig. 17 The energy-wave number characteristic (schematic).

Fig. 18 Positions of q_o and $2k_F$ of divalent and trivalent metals, together with structural weights of fcc, hcp and bcc structures, all in units of $2\pi/A$.

Fig. 19 Band structure energy in 8 cone model. (Weaire, private communication).

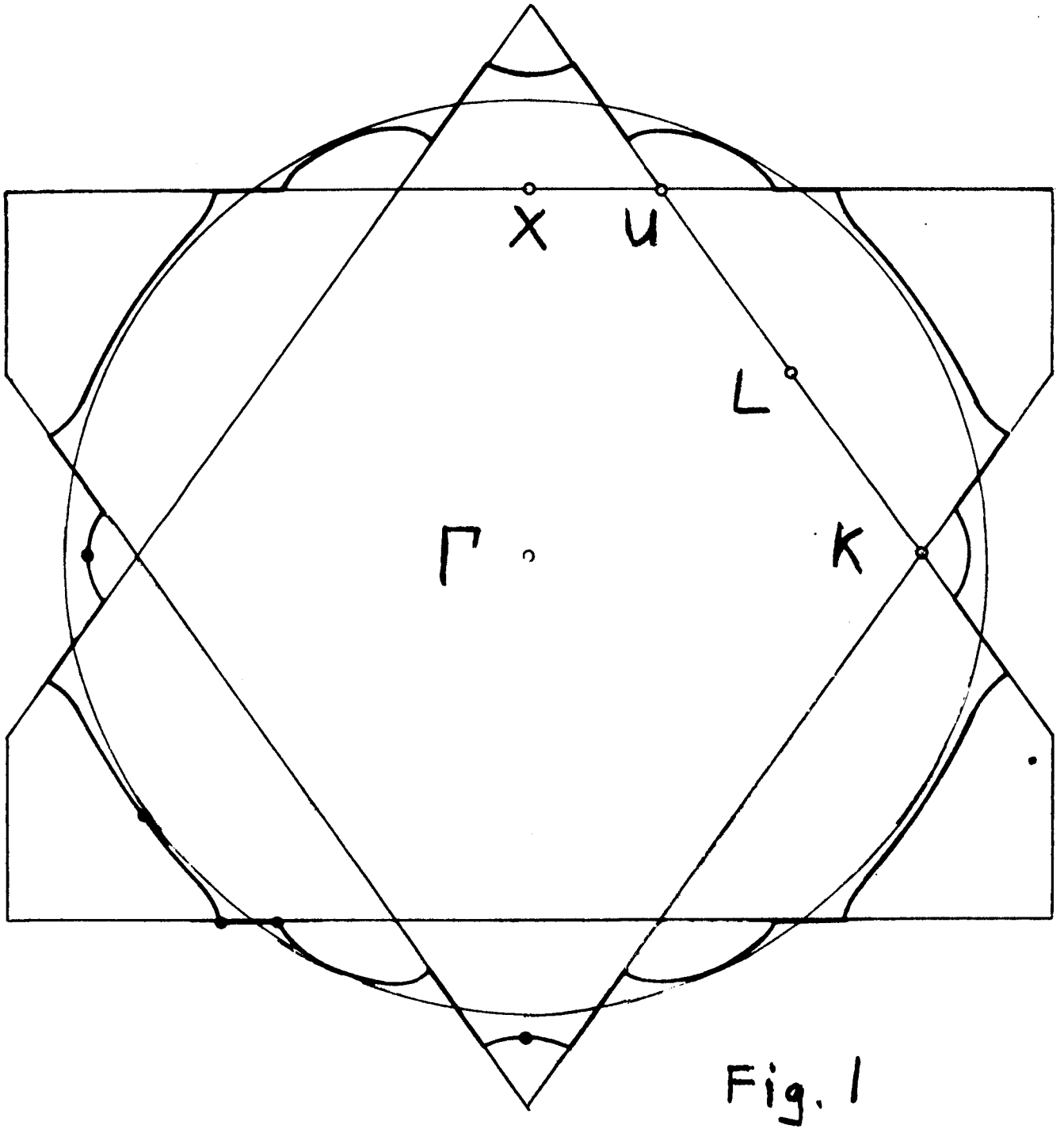

Fig. 1

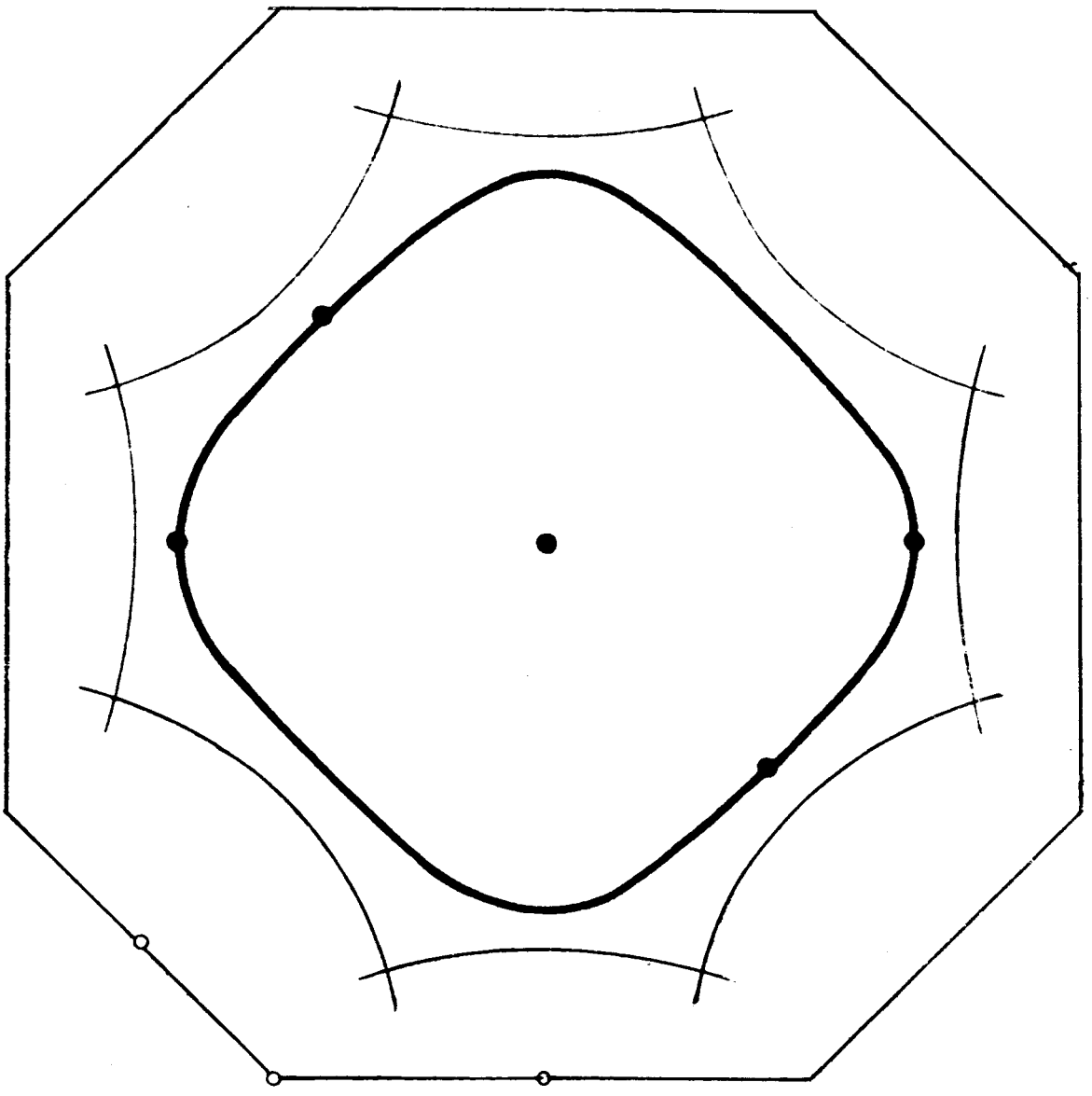

Fig 2a

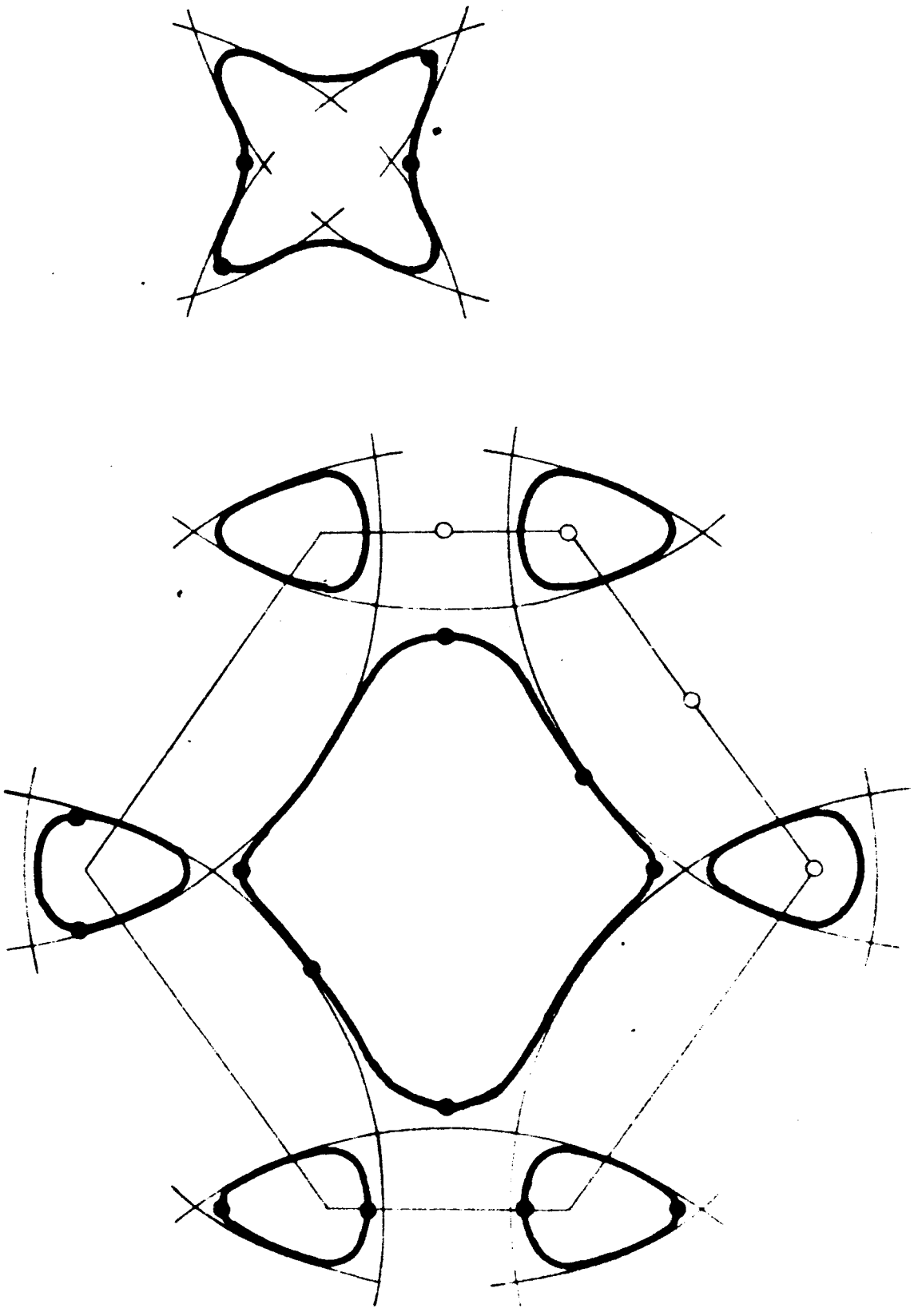

Fig 2b

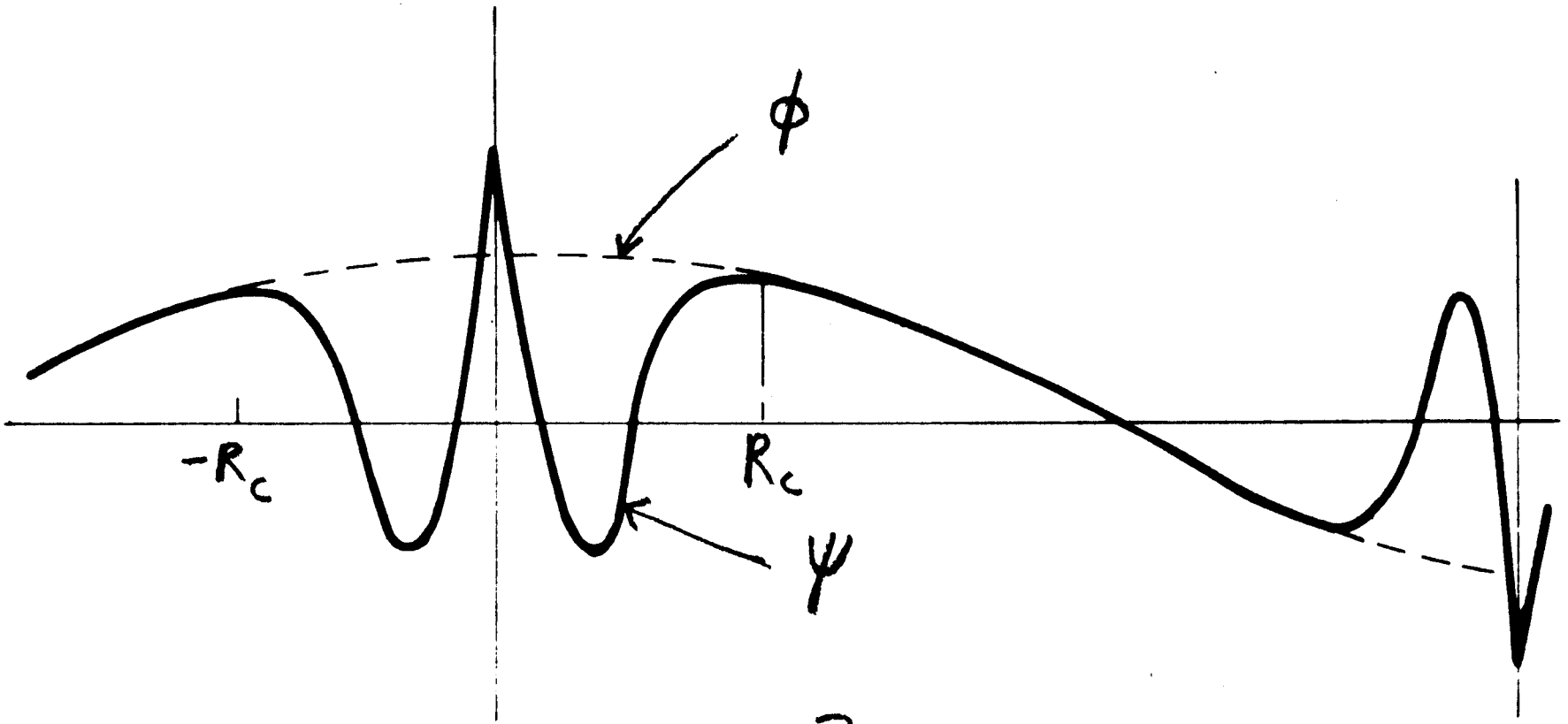

Fig. 3

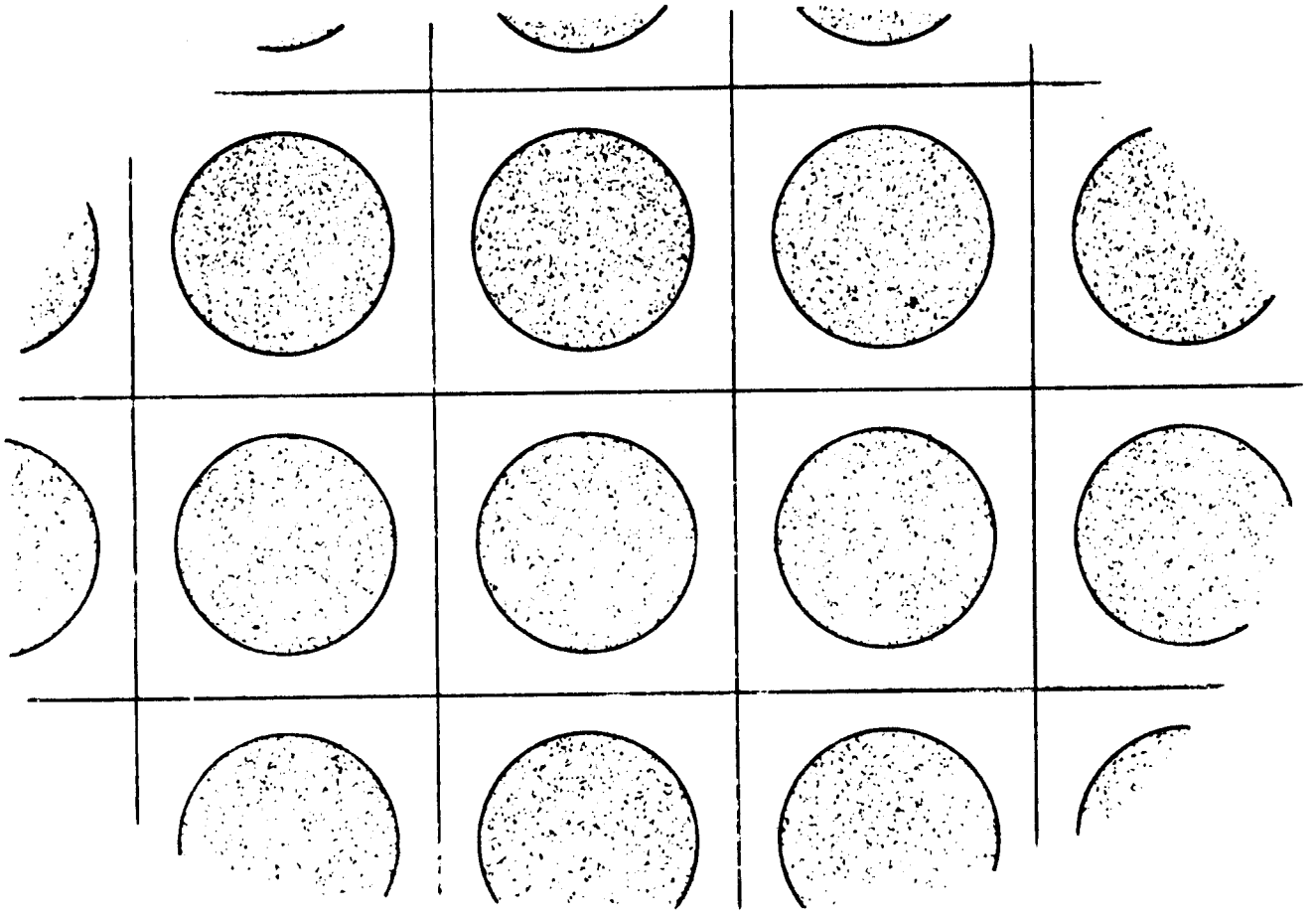

Fig. 4

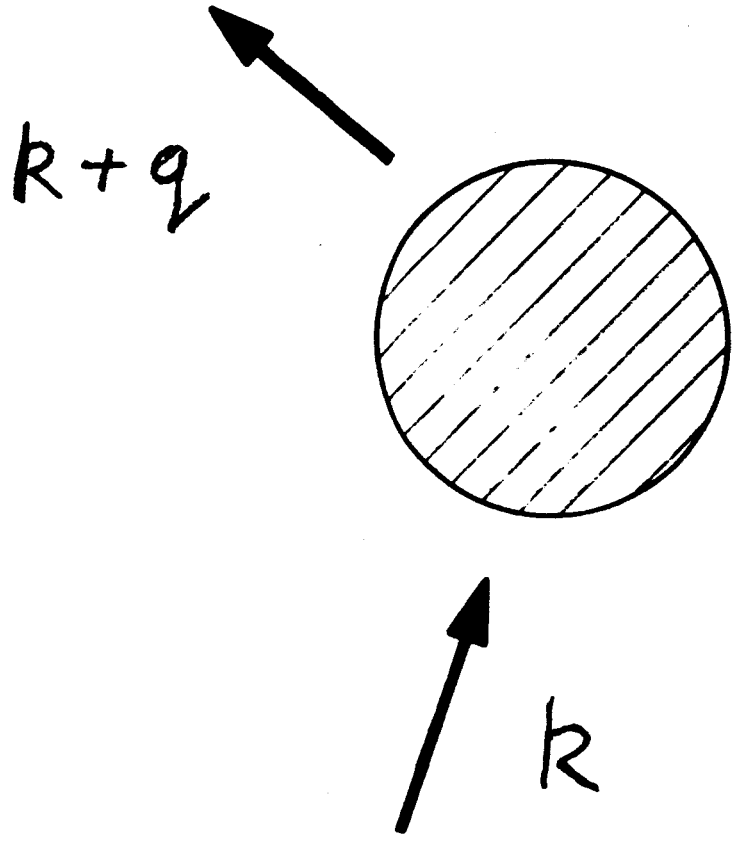

Fig. 5

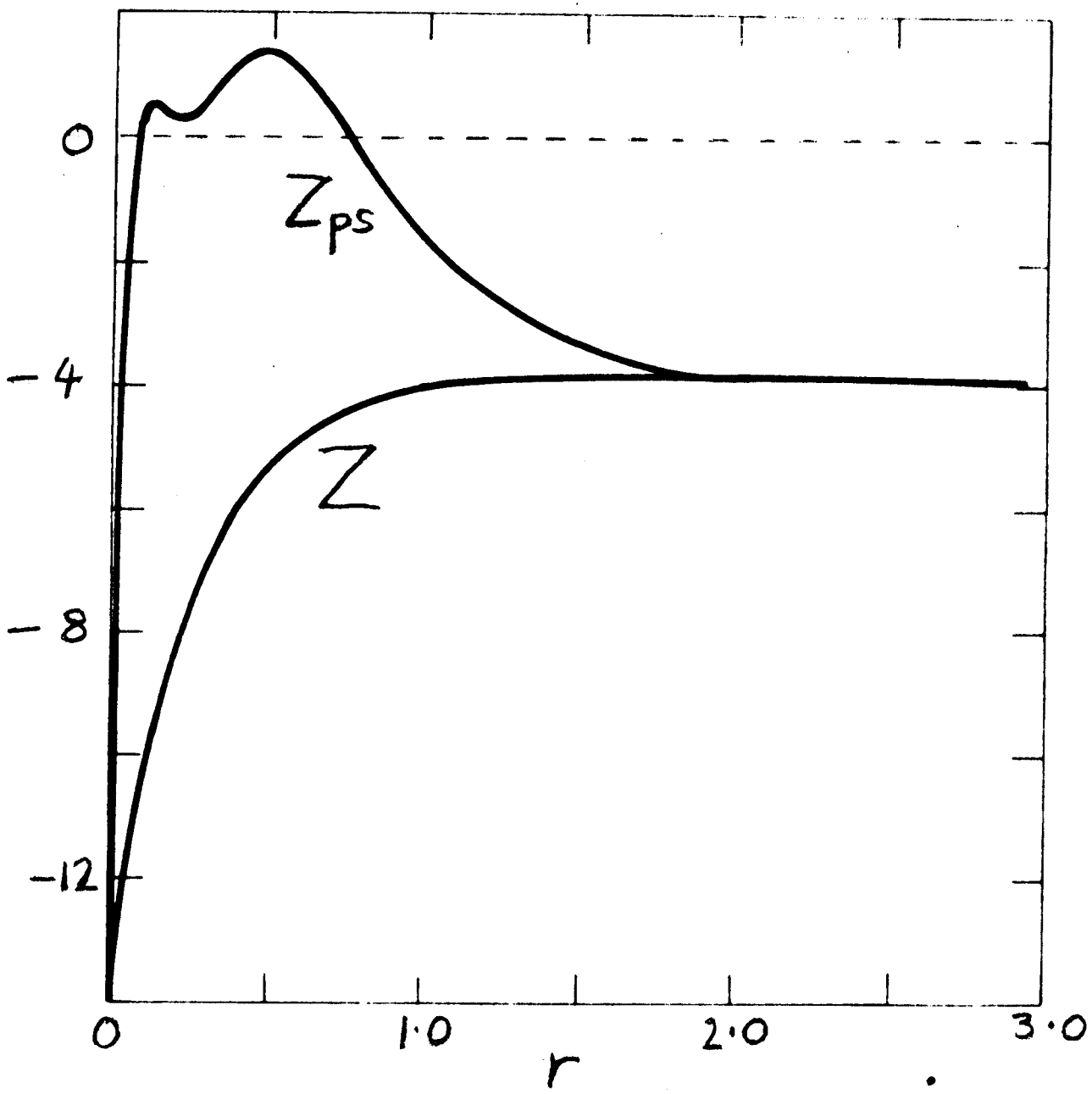

Fig. 6

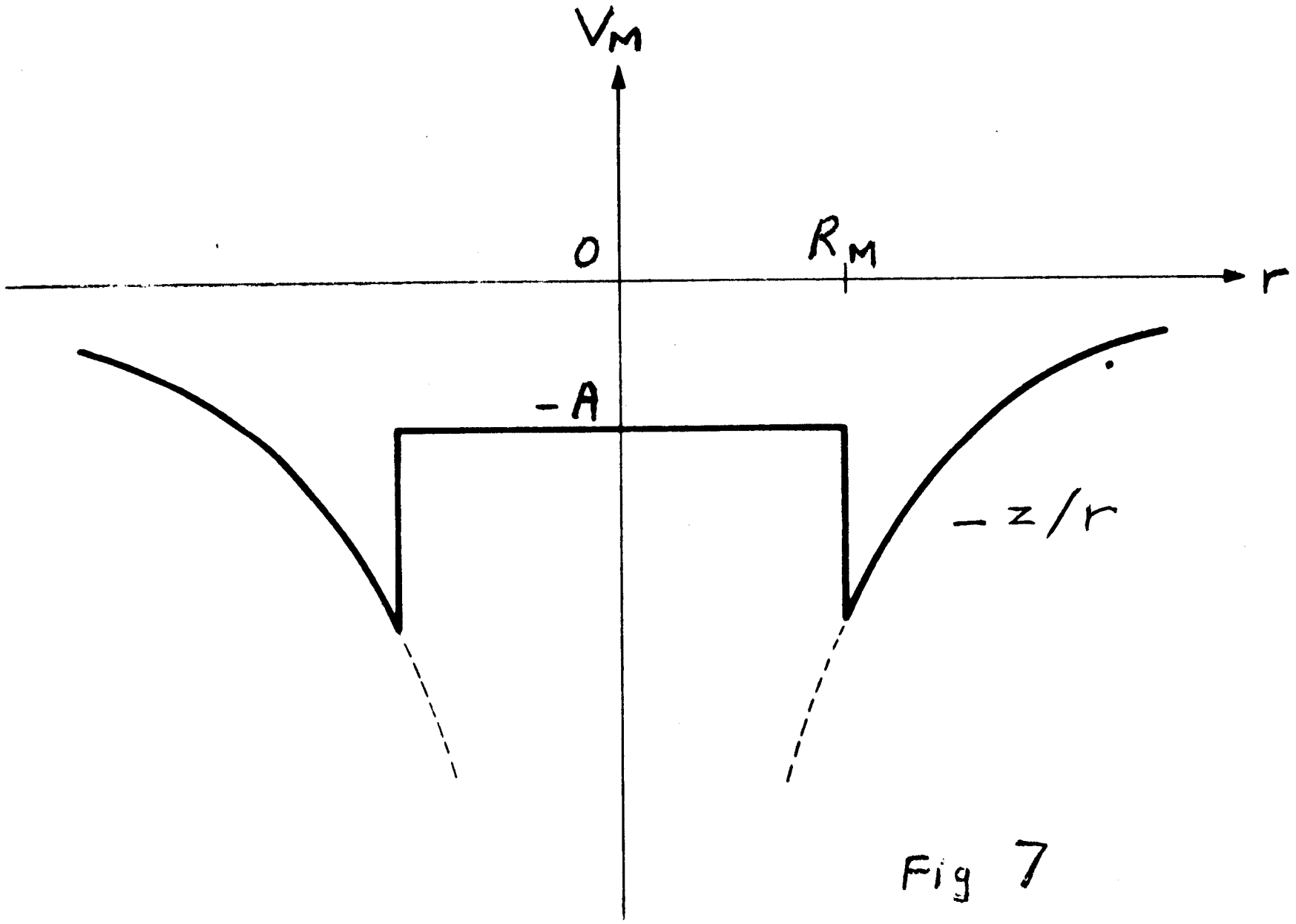

Fig 7

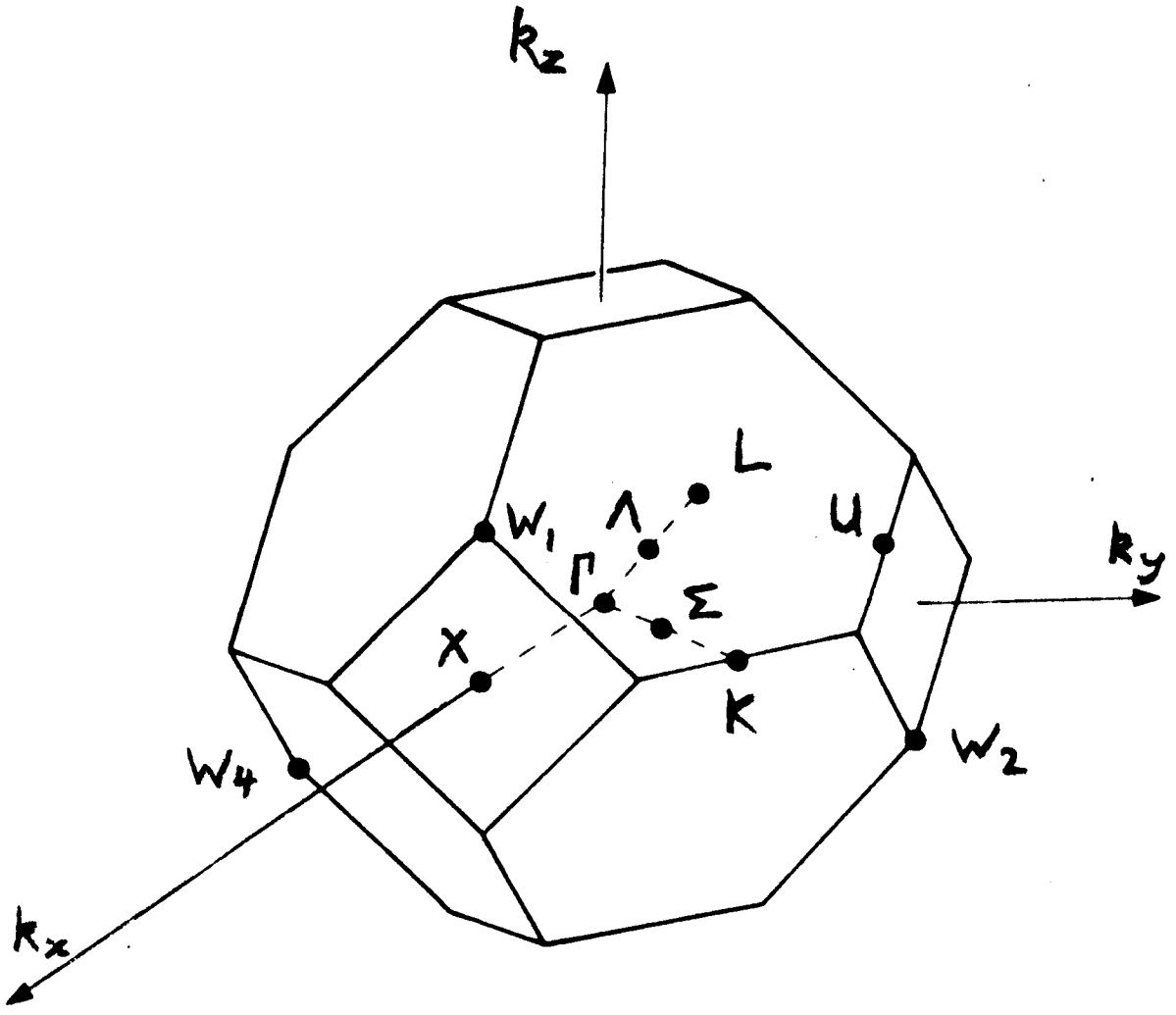

Fig 8

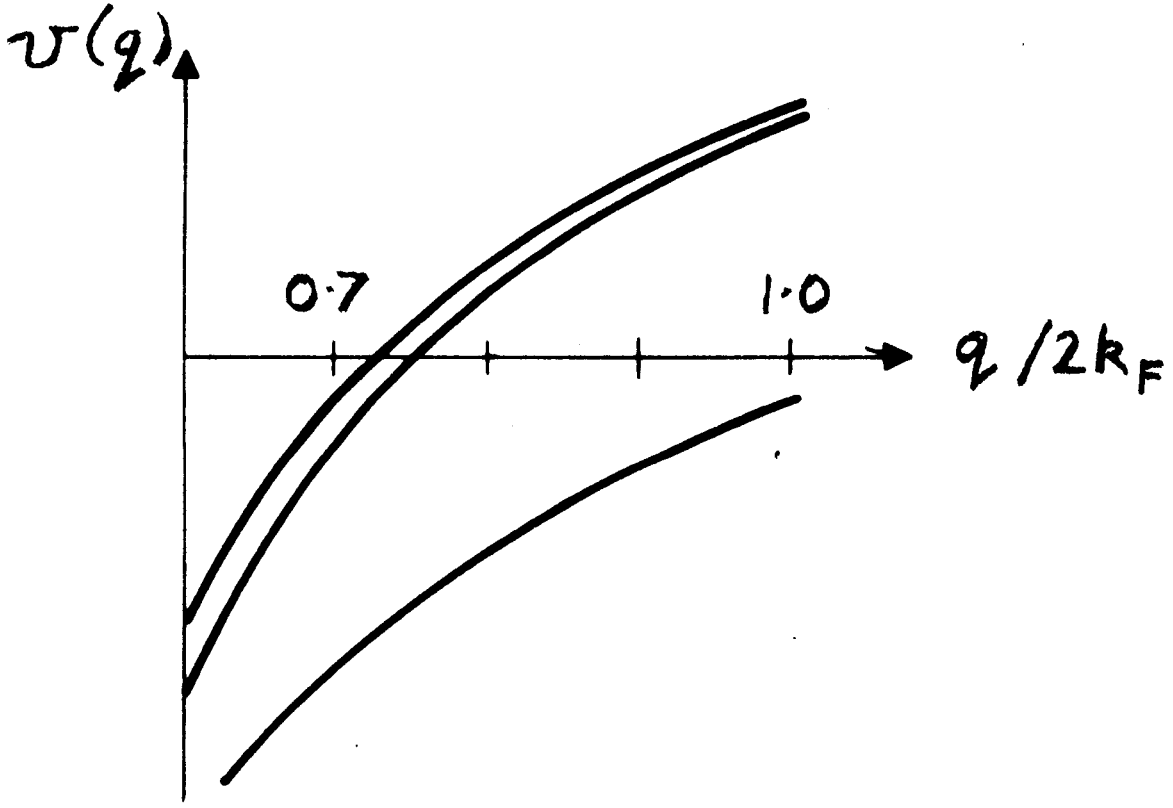

Fig 9

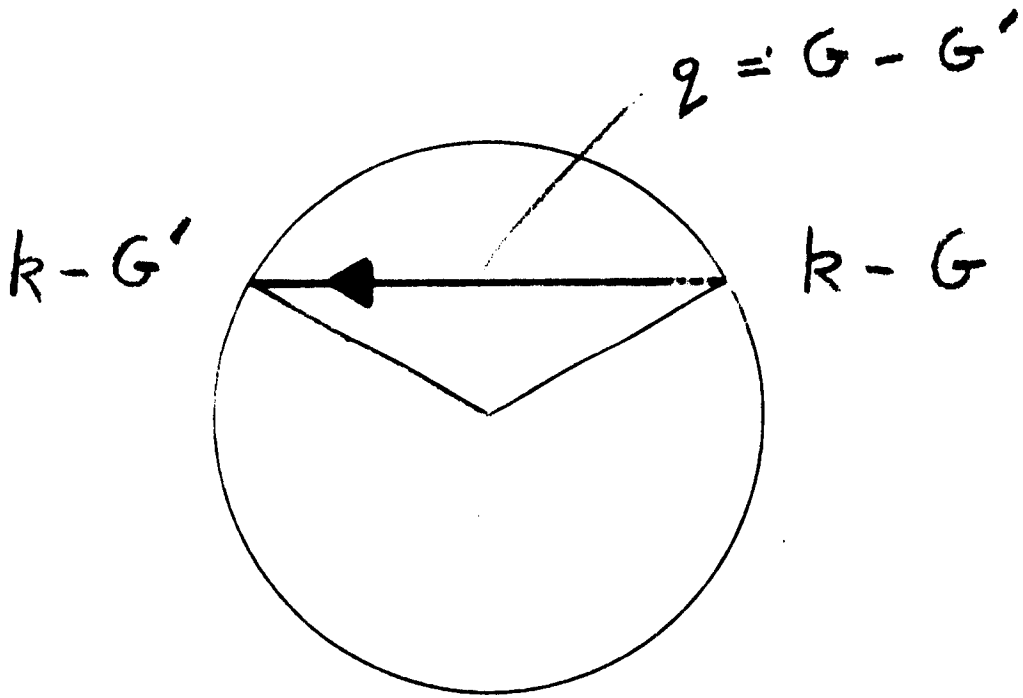

Fig 10

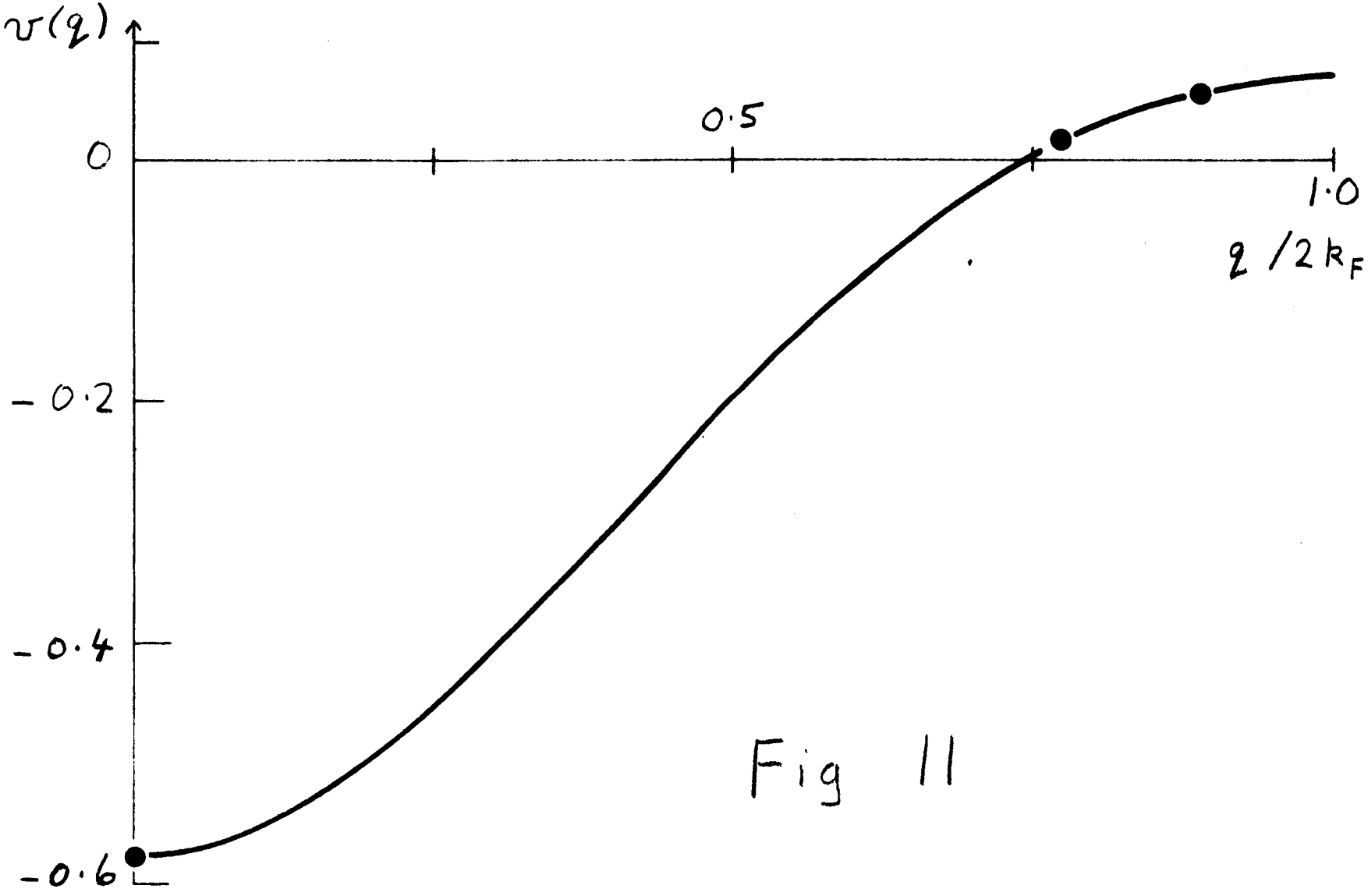

Fig 11

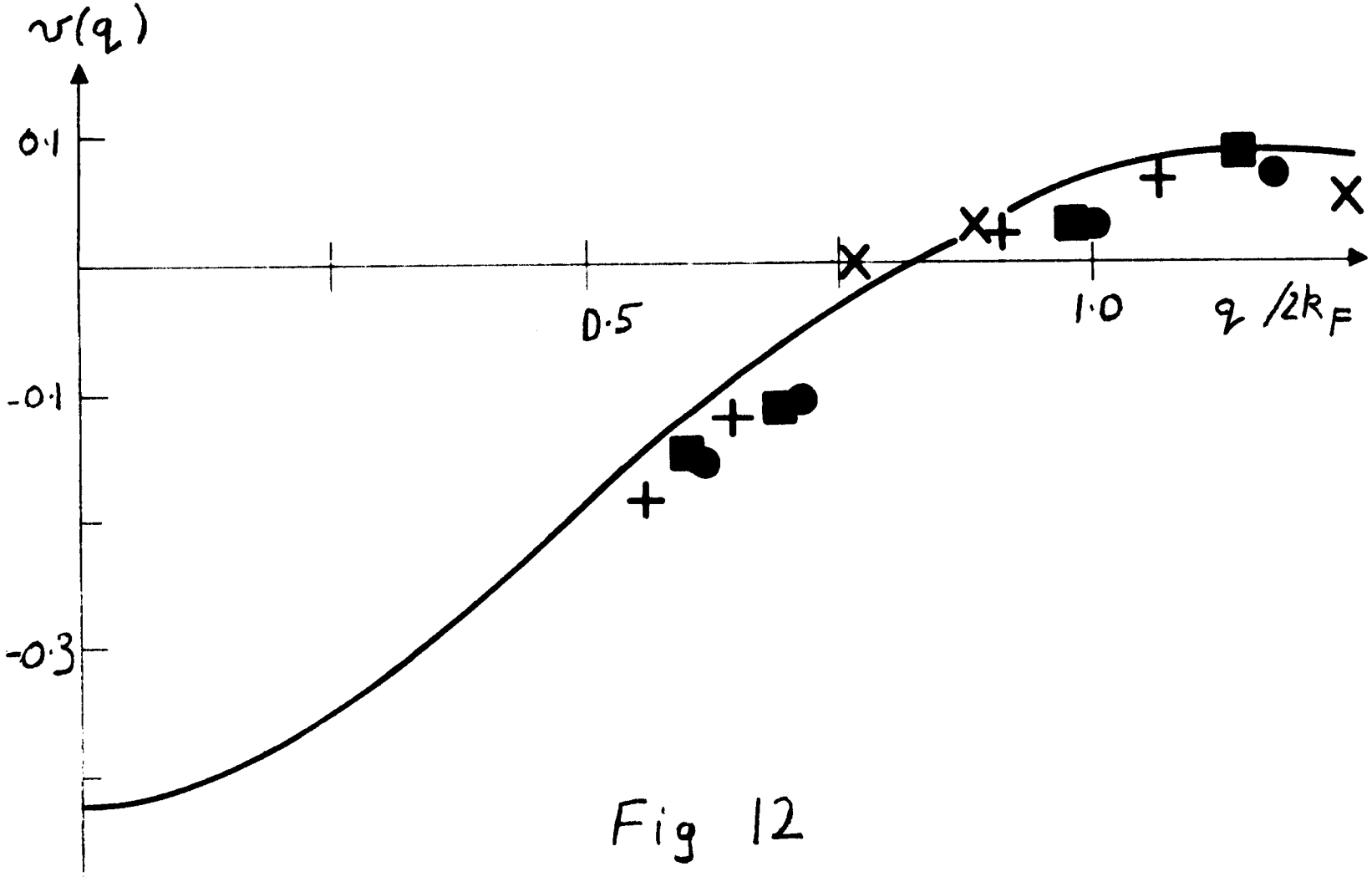

Fig 12

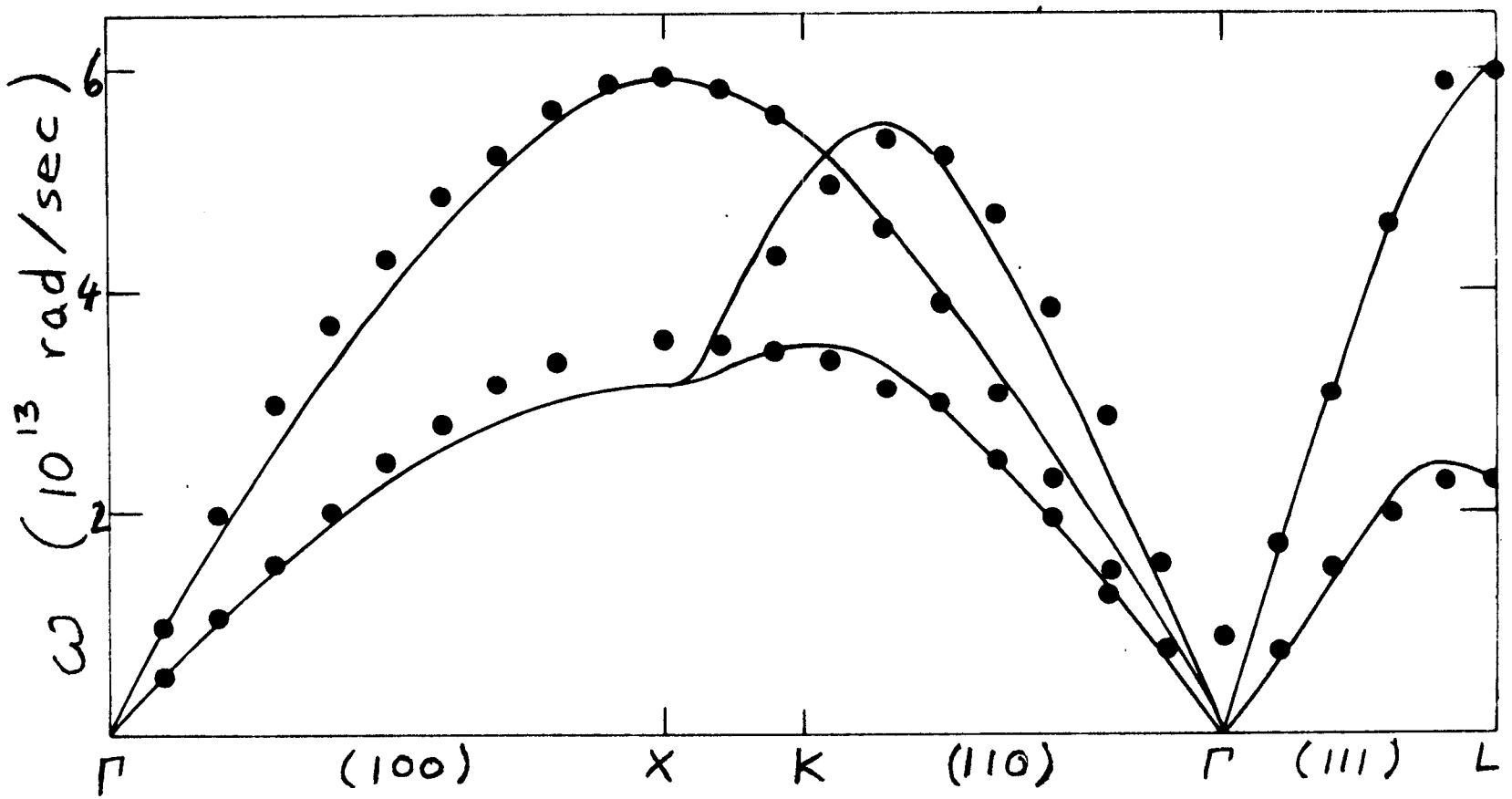

Fig 13

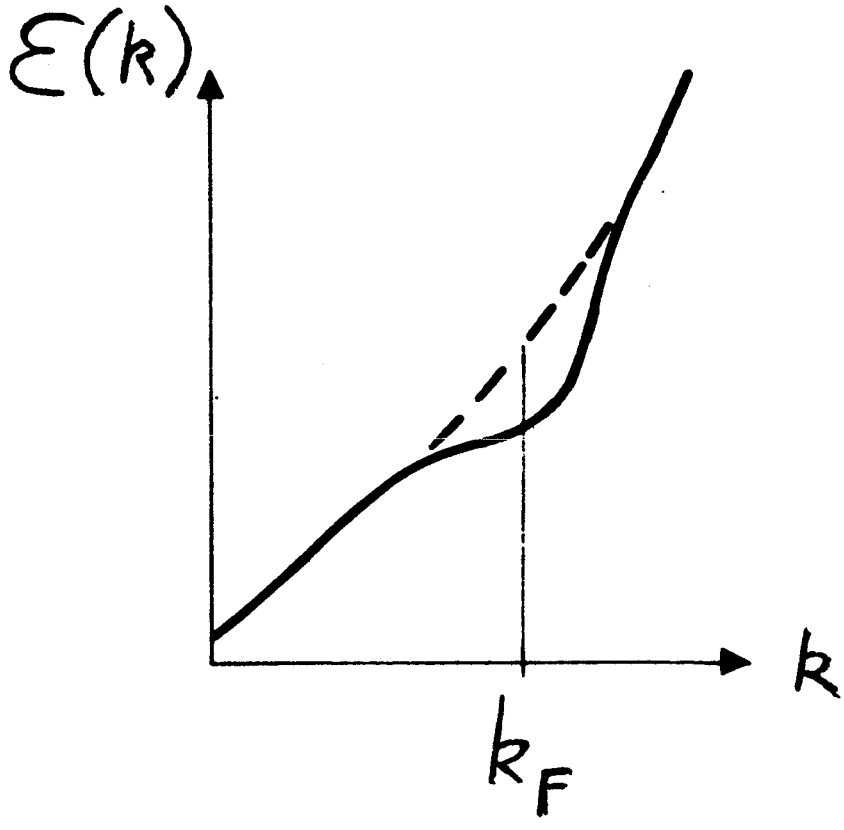

Fig. 14

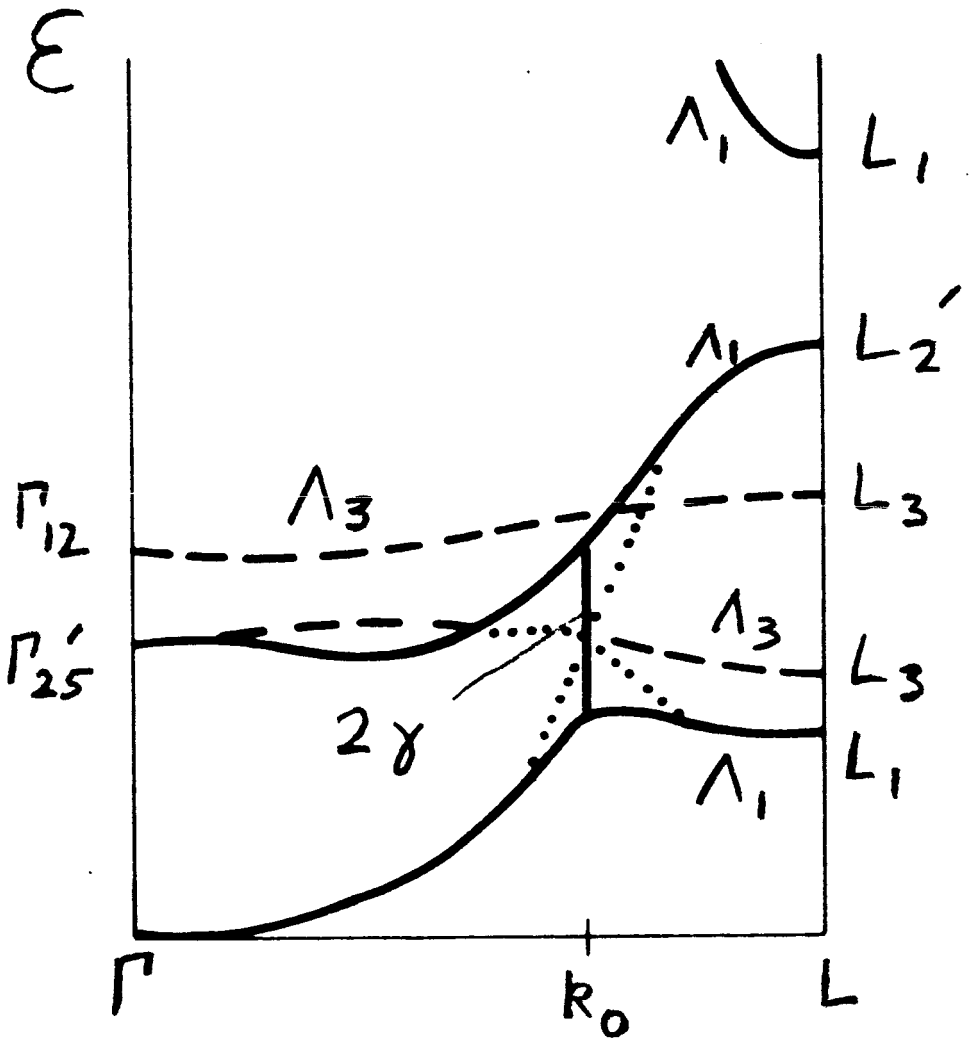

Fig 15

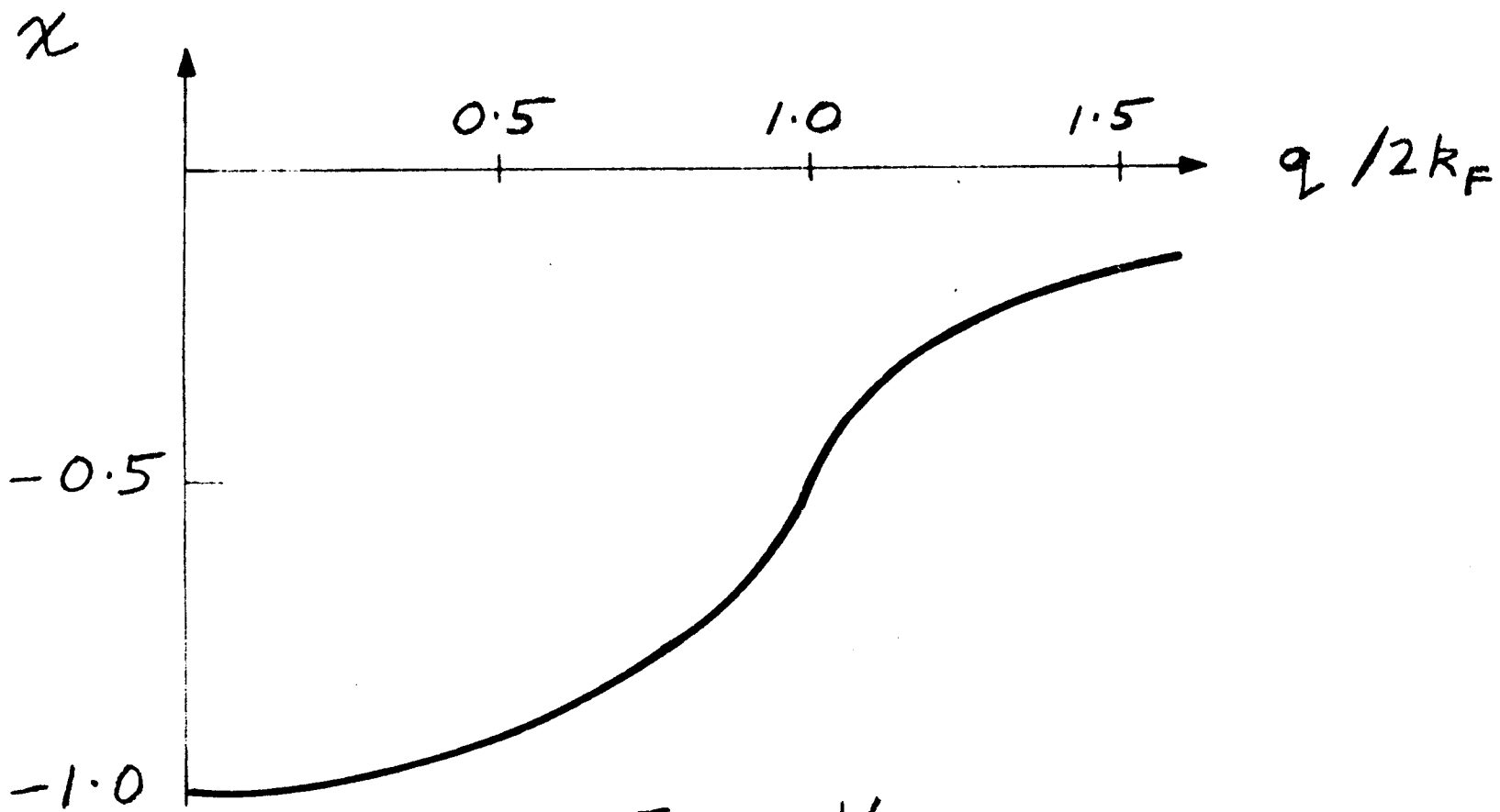

Fig 16

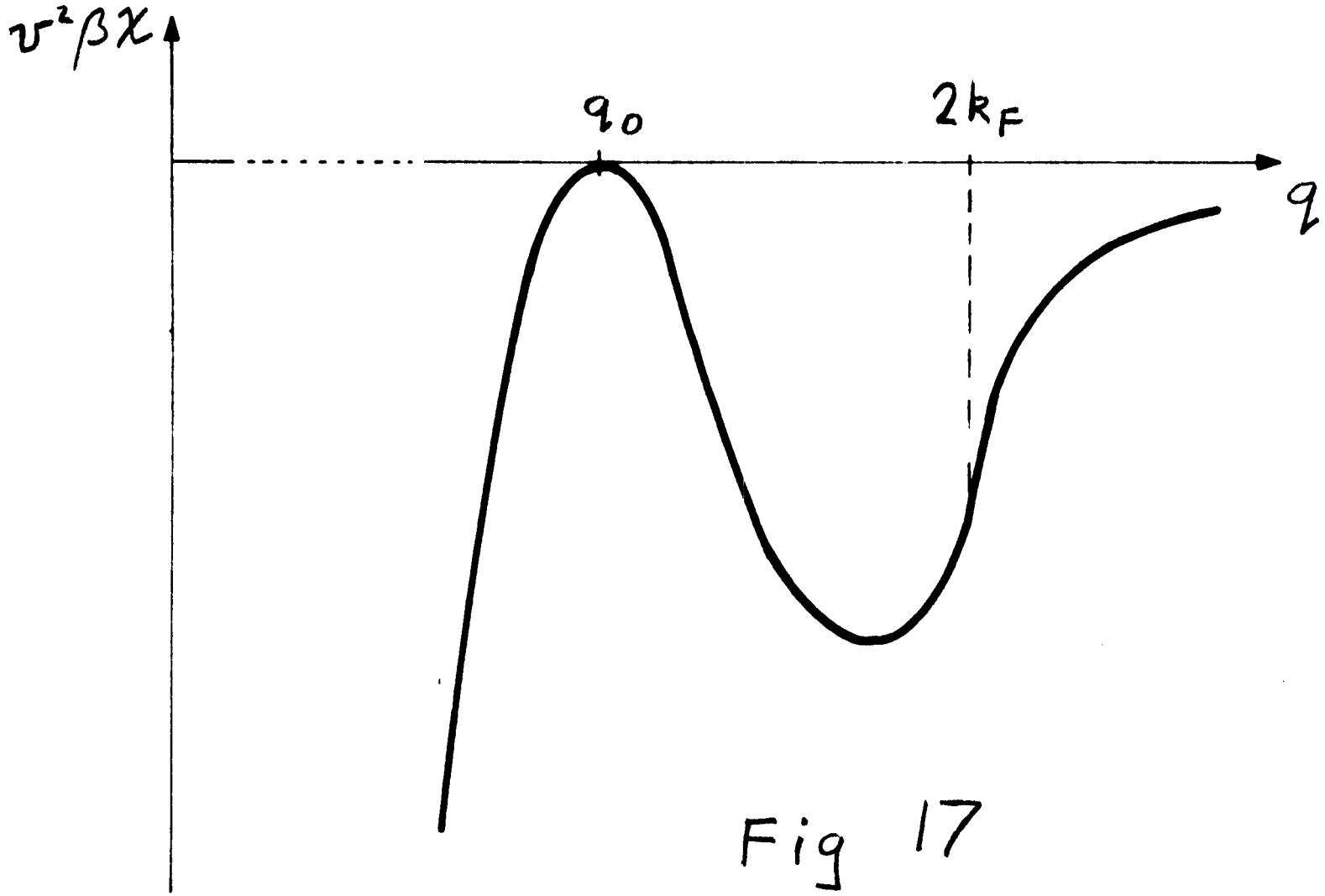

Fig 17

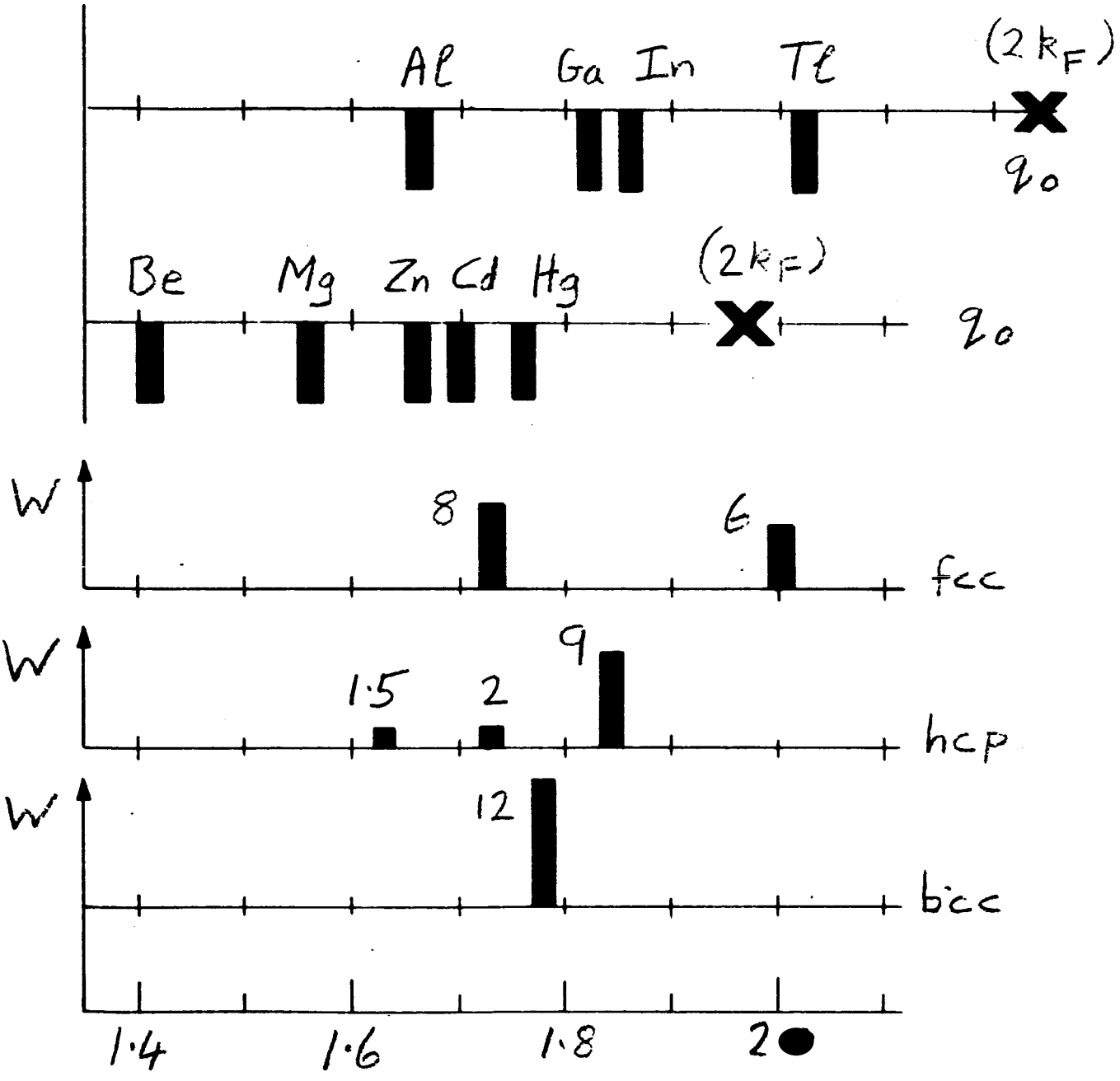
Al
Ga
In
Tl
$(2k_F)$
q_0
Be
Mg
Zn
Cd
Hg
$(2k_F)$
q_0
W
8
6
fcc
W
1·5
2
9
hcp
W
12
bcc
1·4
1·6
1·8
2

Fig 18

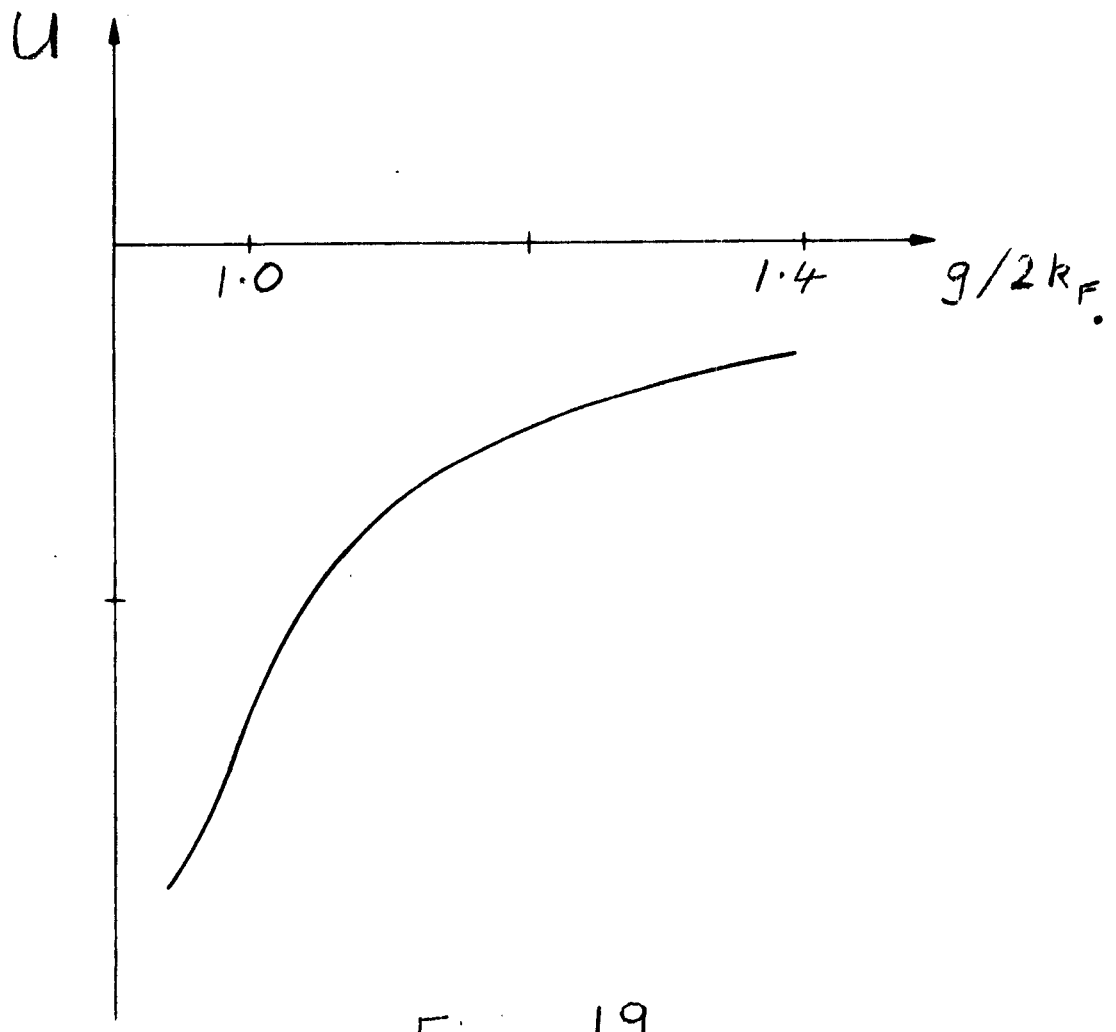

Fig. 19